

Cite this: *Dalton Trans.*, 2014, **43**, 3815

Received 19th December 2013,  
Accepted 13th January 2014  
DOI: 10.1039/c3dt53570c  
[www.rsc.org/dalton](http://www.rsc.org/dalton)

## Dynamic heteroleptic metal-phenanthroline complexes: from structure to function†

Manik Lal Saha, Subhadip Neogi and Michael Schmittel\*

Dynamically heteroligated metal centres are auspicious platforms to access multicomponent supramolecular systems, the latter showing unique structures, amazing properties and even emergent functions. The great potential of heteroleptic complexes has materialised after the development of appropriate strategies that warrant quantitative formation in spite of the dynamic character. In this perspective, we discuss our endeavours at developing various heteroleptic self-assembly protocols based on sterically bulky 2,9-diarylphenanthrolines and our work toward self-sorted multicomponent architectures and assemblies with new and useful functions.

## 1. Introduction

Nature masterfully employs *self-assembly* and *self-organisation* in combination with *self-sorting* for constructing the elegant and intricate molecular machinery from which life is built on our planet.<sup>1</sup> For instance, all cellular devices, such as ribosomes, mitochondria and many smaller multicomponent

enzyme complexes, are made by arranging a multitude of prefabricated covalent building blocks in a proper spatial and functionally active arrangement through noncovalent interactions. As a result, heteroaggregates are at the centre of many specific biological functions, signalling cascades and feedback protocols. It is thus of no surprise that the development of approaches to intricate heteroaggregates in a holistic manner has turned into an attractive research area within *abiological self-assembly*.<sup>2</sup> The latter has already experienced an *ontogenetic* growth, starting from magnificent nanoscale topologies<sup>3</sup> to host-guest chemistry,<sup>4</sup> artificial molecular machines,<sup>5</sup> and smart materials.<sup>6</sup> As a result, contemporary self-assembly has evolved as a broad multidisciplinary domain that provides a fertile ground for breathtaking research.<sup>7</sup>

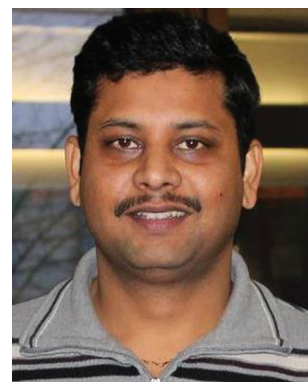
Center of Micro and Nanochemistry and Engineering, Department of Chemistry and Biology, Organische Chemie I, Universität Siegen, Adolf-Reichwein-Str. 2, D-57068 Siegen, Germany. E-mail: schmittel@chemie.uni-siegen.de

†The present review is dedicated to Prof. em. Dr H. D. Lutz (Siegen) on the occasion of his 80<sup>th</sup> birthday.



Manik Lal Saha

Manik Lal Saha was born in 1986 in West Bengal, India. He received his B.Sc. (Honours) in Chemistry from University of Calcutta (India) in 2006. After finishing his M.Sc. from the Indian Institute of Technology Kanpur in 2008, he joined Prof. Schmittel's group at the University of Siegen (Germany). He is currently working towards his PhD on the synthesis of self-sorted multicomponent architectures.



Subhadip Neogi

Subhadip Neogi received his B.Sc. in Chemistry from University of Burdwan (India) and M.Sc. from Banaras Hindu University (India). He obtained his Ph.D. from the Indian Institute of Technology Kanpur in 2008. After completing Humboldt postdoctoral research in Germany with Prof. Michael Schmittel at the University of Siegen, he joined the Department of Chemistry, Indian Institute of Technology Kanpur as a postdoctoral research fellow. His research interests focus on multicomponent supramolecular assemblies and organic-inorganic hybrid porous materials.



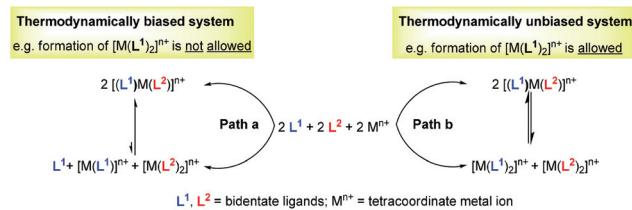


**Fig. 1** Thermodynamic bias to control the heteroleptic complex  $[(L^1)M(L^2)]^{n+}$  formation over that leading to homoleptic complexes  $[M(L^1)_2]^{n+}$  and  $[M(L^2)_2]^{n+}$ .

For example, over the last two decades, *metallosupramolecular* self-assembly<sup>8</sup> has materialised as a promising research area for the synthesis of well-defined, discrete two- and three-dimensional nano-architectures. Despite the notable wealth of the known nano-architectures, nearly all systems comprise only two different components – a ligand and a metal ion – and thus are *homoleptic* in nature and suffer from a lack of diversity.<sup>9</sup> To our understanding, heteroleptic architectures are less frequently targeted due to the lack of convincing strategies that enable the exclusive formation of dynamic *mixed complexes* and that require control over the concurrent binding of two or more different freely exchanging ligands at a single metal centre.<sup>10</sup> For instance, even in the simplest possible case, *i.e.* starting with an equimolar mixture of two ligands and one metal ion (Fig. 1, path b), one would risk the parallel formation of two homoleptic complexes,  $[M(L^1)_2]^{n+}$  and  $[M(L^2)_2]^{n+}$ , along with the desired mixed complex  $[(L^1)M(L^2)]^{n+}$ . Clearly, in such set-ups, labile metal complexes allow very rapid ligand exchange reactions, thus counteracting the clean formation of a heteroleptic complex in solution.

To drive any dynamic heteroaggregation to completion one needs to impose a sizeable thermodynamic bias in the mixed complex as compared to the homoleptic alternatives (Fig. 1, path a). In this respect, chemists often rely on *maximum site occupancy*, requiring optimal saturation of all donor (ligand)

and acceptor (metal-ion) sites while matching all stereochemical requirements.<sup>10,11</sup> In principle, if one is able to suppress formation of at least one of the homoleptic combinations, *e.g.*  $[M(L^1)_2]^{n+}$  (Fig. 1, path a), using the appropriate ligand design, metal coordination specifics and/or stoichiometry bias, then maximum site occupancy will drive quantitative formation of the mixed complex  $[(L^1)M(L^2)]^{n+}$  on enthalpic grounds. Otherwise, energy-rich and coordinatively frustrated entities, *e.g.*  $[M(L^1)]^{n+}$  and  $L^1$ , would form along with  $[M(L^2)_2]^{n+}$  and  $[(L^1)-M(L^2)]^{n+}$ . Over the years, Sauvage,<sup>12</sup> Lehn,<sup>13</sup> Fujita,<sup>14</sup> Stang,<sup>15,16</sup> Schmittel<sup>17</sup> and others<sup>18,19</sup> have used and refined the principle (Fig. 2) in the context of metal-coordination driven dynamic heteroleptic architectures.<sup>10</sup> For example, Sauvage implemented topological constraints at one ligand preventing formation of its bishomoleptic assembly, while Schmittel precluded one of the bishomoleptic complexation motifs due to steric shielding. In other cases (Fig. 2), where both bishomoleptic complexes are equally possible, the hetero-selectivity is attained either by applying a well-balanced steric programming (Fujita and Stang), capitalising on the coordination specifics of penta-coordinating copper(II) ions (Lehn) or profiting on the charge separation effect (Stang).

Undoubtedly, considering the minute number of well-established heteroligation protocols (Fig. 2), the vision of setting up functional assemblies that replicate even partly some complex biological function remains quite far-fetched. To mimic biological machineries, however, the required *multicomponent* assemblies need to possess several *orthogonal* homo- and/or hetero-recognition motifs<sup>20</sup> that precisely cooperate with each other.<sup>21</sup> For this, one may apply the same strategy as that used by nature: amalgamate self-assembly and *self-sorting*<sup>22</sup> protocols to integrate different subunits into the final architecture with precise spatial/positional and constitutional control. Hence, there has been, in recent years, a renewed quest for deeper understanding of the various concepts which are vital to multicomponent assembly such as *orthogonality* in coordination motifs,<sup>20</sup> *completive* and *integrative* self-sorting,<sup>22c</sup> cooperative and allosteric effects, *etc.*<sup>21</sup>

This perspective describes our efforts and advancement in understanding and exploring the concepts of dynamic heteroleptic complexation using 2,9-diarylphenanthrolines as the key building blocks (Fig. 2). In the subsequent sections, we will discuss the rational design and the ensuing synthesis of heteroleptic assemblies, thereafter the blending of optimised heteroleptic motifs into multicomponent self-sorted aggregates and finally architectures that offer new and useful functions.



Michael Schmittel

Michael Schmittel studied chemistry and French in Freiburg and Paris. After a postdoctoral stay in Rochester/USA and habilitation at the University of Freiburg, he joined the University of Würzburg as an associate professor in 1993 and since 1999 holds a Chair in Organic Chemistry at the University of Siegen. His broad interests, published in ca. 230 papers and one textbook, cover research areas as diverse as diradical cyclisations, metallocsupramolecular coordination chemistry, lab-on-a-molecule chemosensors and, starting recently, (supra)molecular machines and nanoswitches.

## 2. Our heteroleptic toolkits and polynuclear complexes derived therefrom

In 1997, our studies on metal phenanthroline complexes revealed an interesting behaviour (Scheme 1a).<sup>23</sup> An equimolar mixture of  $Cu^+$  and the two phenanthrolines **1**, **2** at equilibrium did not afford a statistical mixture of all three



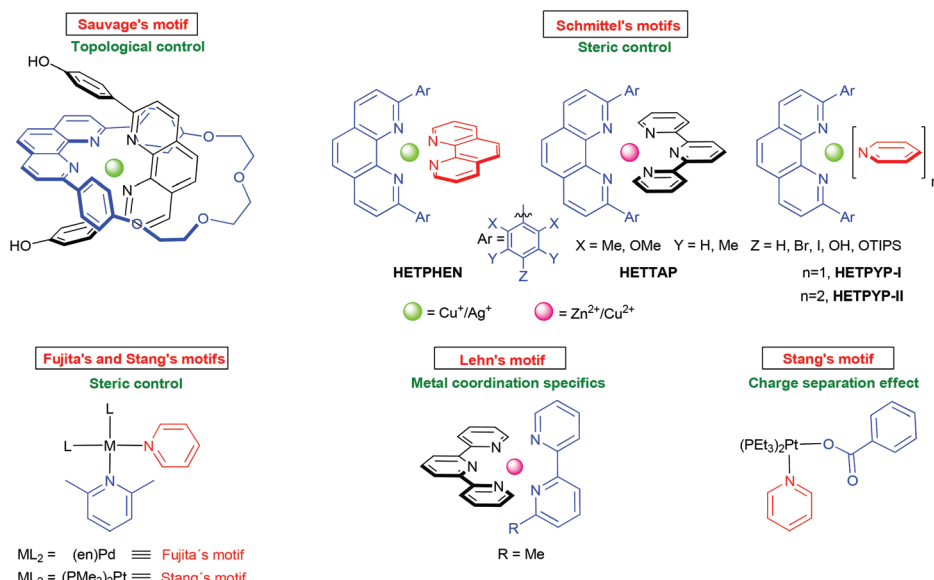


Fig. 2 Strategies to quantitatively prepare mixed metal complexes in solution.

possible complexes 3–5 (Scheme 1a). Instead, only the complexes **3** =  $[\text{Cu}(\mathbf{1})_2]^+$  and **4** =  $[\text{Cu}(\mathbf{1})(\mathbf{2})]^+$  were furnished in a ratio of 2 : 1, suggesting that complex **3** with its four intramolecular  $\pi$ – $\pi$  stacking interactions is thermodynamically favoured over the heteroleptic complex **4** (two  $\pi$ – $\pi$  stacking interactions) and homoleptic complex **5** =  $[\text{Cu}(2)_2]^+$  (zero  $\pi$ – $\pi$  stacking interactions). The thermodynamics of this copper(i) complex equilibration is qualitatively reflected by the energy levels depicted in Scheme 1b. Clearly, to realise exclusive formation of the desired heteroleptic complex, one needs simply to increase the barrier for the  $[\text{Cu}(\mathbf{1})(\mathbf{2})]^+ \rightarrow [\text{Cu}(\mathbf{1})_2]^+$  transformation. At this juncture, we reasoned that a sterically shielded 2,9-diaryl-phenanthroline ( $\text{phen}_{\text{Ar}2}$ ) is a highly promising candidate (Scheme 1c), because its bishomoleptic copper complex should be impossible applying a proper balance of steric and electronic effects. Indeed, the combination of various  $[\text{Cu}(\text{phen}_{\text{Ar}2})]^+$  motifs with a sterically unpretentious counter-ligand, used at correct stoichiometry, provided exclusively the heteroleptic complex that is driven by maximum site occupancy (*vide supra*). Over the years, we have refined this approach for various ligands and metal ions and used it for constructing a rich variety of dynamic oligonuclear structures. In the following, we will portray the different protocols and some interesting architectures derived therefrom.

### 2.1. HETPHEN concept

The HETPHEN complexation is a three-component assembly strategy developed for the selective formation of HETeroleptic bis-PHENanthroline metal complexes (Scheme 1c and Fig. 3).<sup>23</sup> Over the years, the HETPHEN approach has proved its value in the preparation of heteroleptic mononuclear  $\text{Cu}^{+}$ ,  $\text{Ag}^{+}$ - and  $\text{Zn}^{2+}$ -bisphenanthroline,<sup>24</sup> mixed phenanthroline-2,2'-bipyridine (bipy) complexes,<sup>25</sup> and a rich variety of supramolecular polynuclear structures derived therefrom, such as

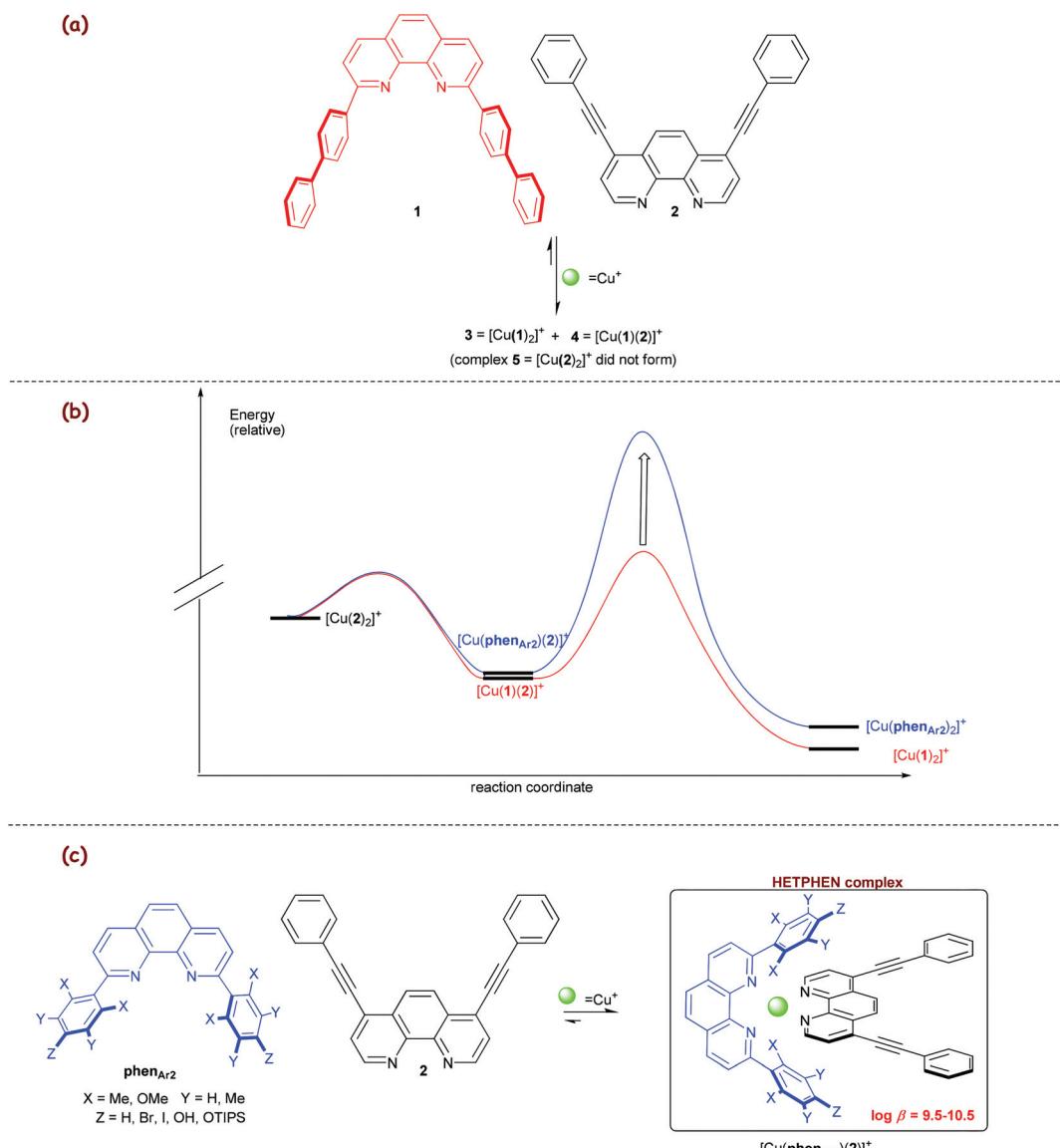
triangles,<sup>26</sup> ring-in-ring assemblies,<sup>27</sup> nanoscaffolds,<sup>28</sup> triple-deckers,<sup>29</sup> nanogrids,<sup>30</sup> nanoracks,<sup>31</sup> porphyrin stacks<sup>32</sup> and nanobaskets.<sup>33</sup> In addition, using a variant of the HETPHEN strategy, we recently developed an access to constitutionally dynamic heteroleptic  $[\text{Cu}(\text{phen}_{\text{Ar}2})(\text{iminopyridine})]^+$  complexes ( $\log \beta \approx 9\text{--}11$ )<sup>34,35</sup> (Fig. 3) through four-component assembly. During those studies, we recognised that the much weaker binding picolinaldehydes, our versatile precursors to iminopyridines, themselves undergo heteroleptic complex formation to  $[\text{Cu}(\text{phen}_{\text{Ar}2})(\text{picolinaldehyde})]^+$  at  $\log \beta \approx 8\text{--}8.5$ .<sup>34c</sup> It is a big advantage of iminopyridine complexes that, due to their high dissociation–association dynamics, overall kinetic barriers in intricate complexation processes are lower than those of the sturdy phenanthroline ligands, an important feature to drive supramolecular exchange and repair processes (*vide infra*).

Based on the efficient repair in constitutionally dynamic iminopyridines and their complexes, we recently realised the formation of the diastereomerically pure heteroleptic metal-organic cage **9**.<sup>34a</sup> Cage **9** was manufactured from the  $C_3$ -symmetric building blocks **6** and **8**. The latter may be used either in the prefabricated form or generated *in situ* from picolinaldehyde and trianiline **7** (Scheme 2).<sup>34a</sup>

### 2.2. HETTAP concept

In 2005, we developed the HETTAP concept (HETeroleptic Terpyridine And Phenanthroline complexation) that allows one to prepare heteroleptic complexes of the type  $[\text{M}(\text{phen}_{\text{Ar}2})\text{-}(\text{terpy})]^{\text{n}+}$  with terpy representing a terpyridine ligand (Scheme 3a).<sup>36</sup> Lately, this concept was extended to constitutionally dynamic heteroleptic  $[\text{M}(\text{phen}_{\text{Ar}2})(\text{diiminopyridine})]^{\text{n}+}$  complexes (Scheme 3b). 2,9-Bis(2,6-dimethoxyphenyl)-1,10-phenanthroline and  $\text{Zn}^{2+}$  ions turned out to be the most suitable combination to accomplish the heteroleptic complexation, as otherwise either diiminopyridines would form





**Scheme 1** (a) Influence of intracomplex  $\pi-\pi$  interactions on copper(i) complex equilibria. (b) Energy diagram depicting the complexation equilibria. (c) The HETPHEN concept.<sup>23</sup>

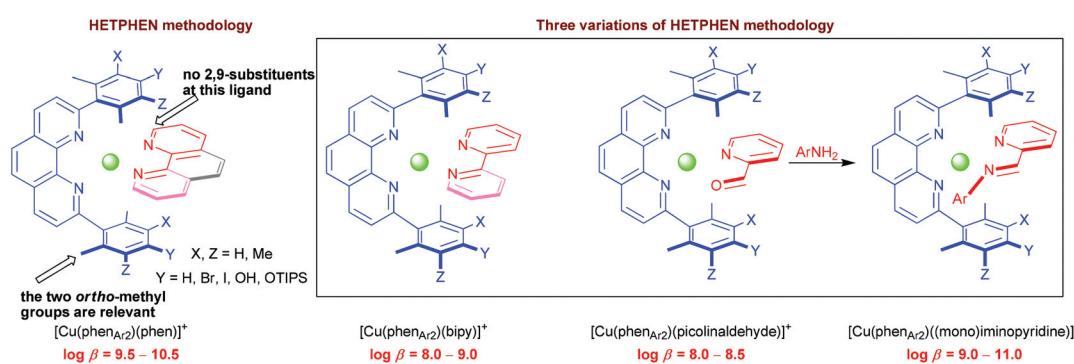
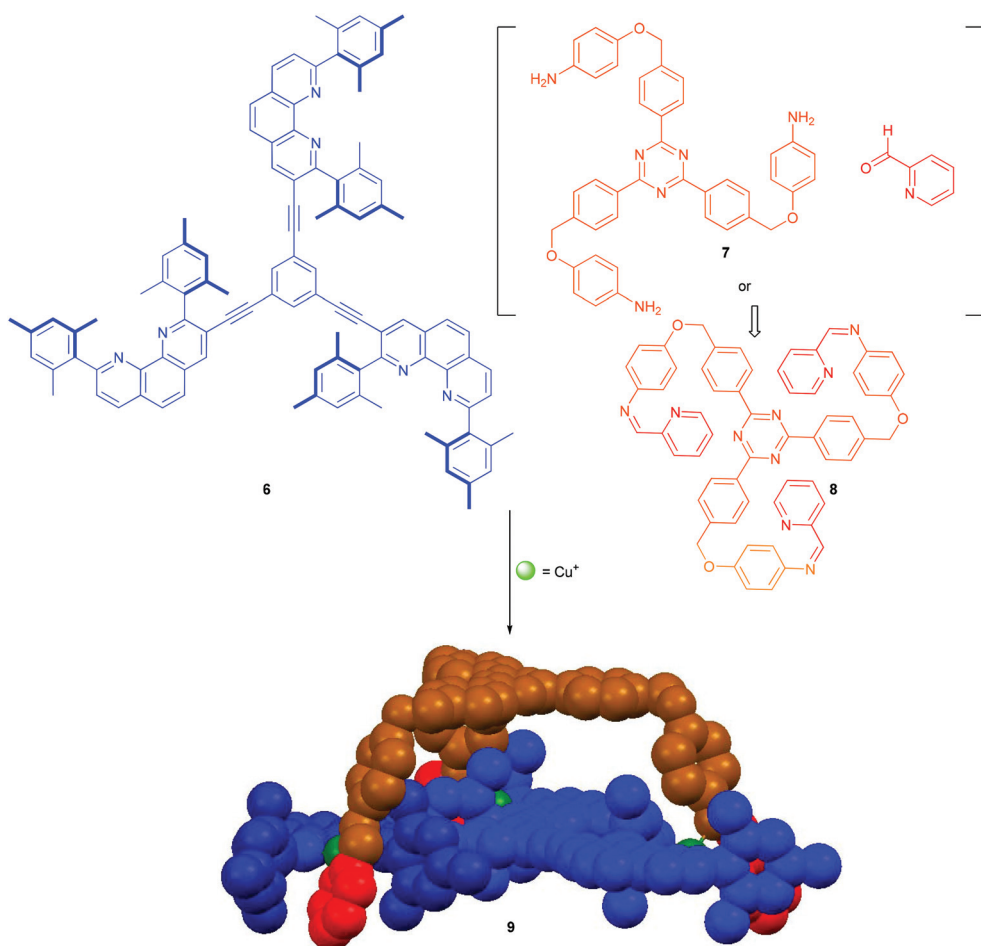


**Fig. 3** Variations in the HETPHEN concept: heteroleptic  $[\text{Cu}(\text{phen}_{\text{Ar}2})(\text{bipy})]^+$ ,<sup>25</sup>  $[\text{Cu}(\text{phen}_{\text{Ar}2})(\text{picolinaldehyde})]^+$  and  $[\text{Cu}(\text{phen}_{\text{Ar}2})(\text{iminopyridine})]^+$  motifs.<sup>34b</sup>



**Scheme 2** Cage structure **9** prepared from the triple-arm tris-iminopyridine **8** and trisphenanthroline **6** by the formation of three  $[\text{Cu}(\text{phen}_{\text{Ar}2})\text{-}(\text{iminopyridine})]^+$  linkages.<sup>34a</sup>

incompletely or the kinetically rather stable hexa-coordinated bis(diiminopyridine) zinc complexes would arise in sizable amounts.<sup>37</sup>

The high reliability of the HETTAP complexation process was demonstrated by preparing a number of supramolecular structures, such as nanoladders,<sup>36</sup> supramolecular dumbbells,<sup>38</sup> molecular-wheels,<sup>39</sup> nano-prisms,<sup>40</sup> isosceles triangles,<sup>41</sup> tweezers,<sup>42</sup> etc. In 2008, we interrogated the approach toward the synthesis of the technomimetic spoked wheel **12**<sup>39</sup> that was prepared by the copper(i)-based self-assembly protocol (Scheme 3c). As depicted in Scheme 3c, the  $D_{6h}$ -symmetric hexakis(terpyridine) **10** acts as a *molecular spoke set* in the structure of **12**, while bisphenanthroline **11** acts as a *rim*. The  $MM^+$  computations on the structure suggested a diameter and a perimeter of 3.9 and 12.3 nm, respectively.

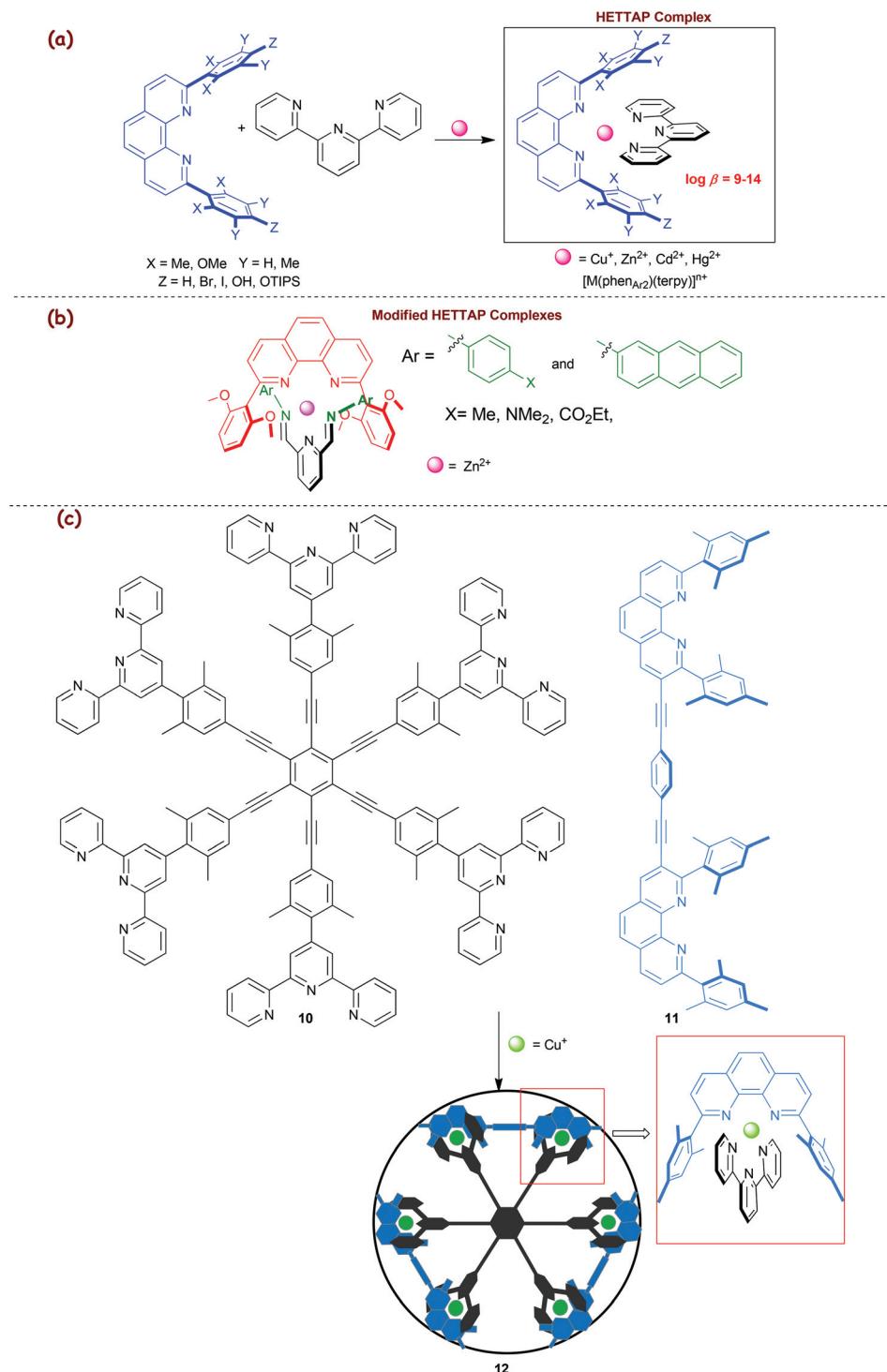
### 2.3. HETPYP concept

In 2009, we added the HETPYP-II concept<sup>43</sup> (HETeroleptic PYridine and Phenanthroline complexation) that allows attachment of two pyridine (py) ligands to a copper(i) centre yielding  $[\text{Cu}(\text{phen}_{\text{Ar}2})(\text{py})_2]^+$  complexes. Lately, the concept has been extended to the HETPYP-I protocol (Scheme 4a),<sup>44,45</sup> opening

the way toward trigonal  $[\text{Cu}(\text{phen}_{\text{Ar}2})(\text{py})]^+$  units. As expected, HETPYP-I complexes ( $\log \beta \approx 8\text{--}8.5$ ) are less stable than their HETPHEN and HETTAP analogues. Nevertheless, this complexation motif has proved its reliability in various supramolecules both in solution and in the solid state.<sup>45a</sup> For instance, various three-component racks, rectangles and trigonal prisms were recently prepared based on the HETPYP-I complexation.<sup>45b</sup> Similarly, the HETPYP-II motif was of use in several 2D and 3D-nanoarchitectures, again both in solution and in the solid state. For example, the aesthetically pleasing and topologically interesting *Borromean cage* **14** was readily prepared from a 1 : 1 mixture of ligand **13** and  $\text{Cu}^+$  ions (Scheme 4b).<sup>43</sup> While the formation of cage **14** is driven by maximum site occupancy and entropic constraints, an analogous cage was even synthesised without the HETPYP control.<sup>18b</sup>

## 3. Multicomponent self-sorted nano-assemblies

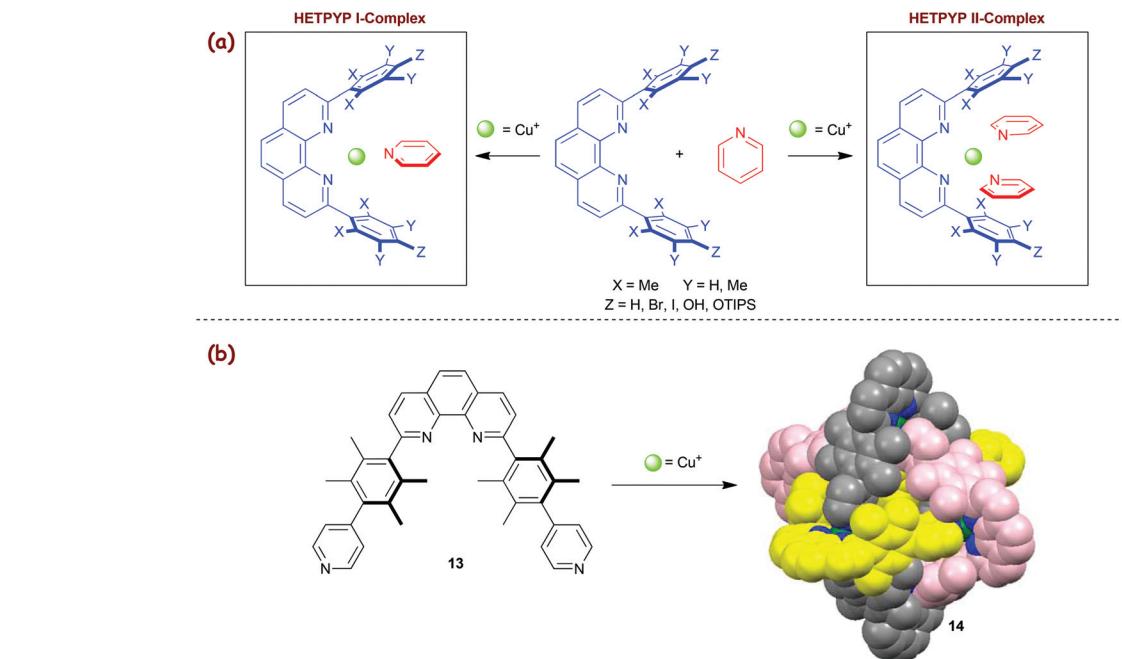
Highly symmetrical architectures from multiple identical building blocks have shown their great utility in various



**Scheme 3** (a) Illustration of the HETTAP approach. (b) Diiminopyridine-based HETTAP complexes. (c) Extension of the HETTAP approach toward the spoked-wheel architecture **12**.<sup>39</sup>

examples of host-guest chemistry.<sup>4,46,47</sup> To reach a higher degree of multifacetedness, though, multiple different components as well as multiple interactions are needed, because the latter may open the venue to functional aggregates with each component adding new functions (*vide infra*).<sup>20</sup> In recent years, thus a good part of our efforts has been devoted to

elaborate new multicomponent self-sorting protocols with a particular focus on *completive* processes (Fig. 4).<sup>22c</sup> In general,  $x$ -fold *completive self-sorting* describes a process in which  $x$  self-assembled entities form from a library containing  $n$  constituents by making quantitative use of all members.<sup>48</sup> With respect to our systems, we desired to amalgamate two or more



Scheme 4 (a) Illustration of HETPYP-I and II approaches. (b) Synthesis of the HETPYP-II based Borromean cage 14.<sup>43</sup>

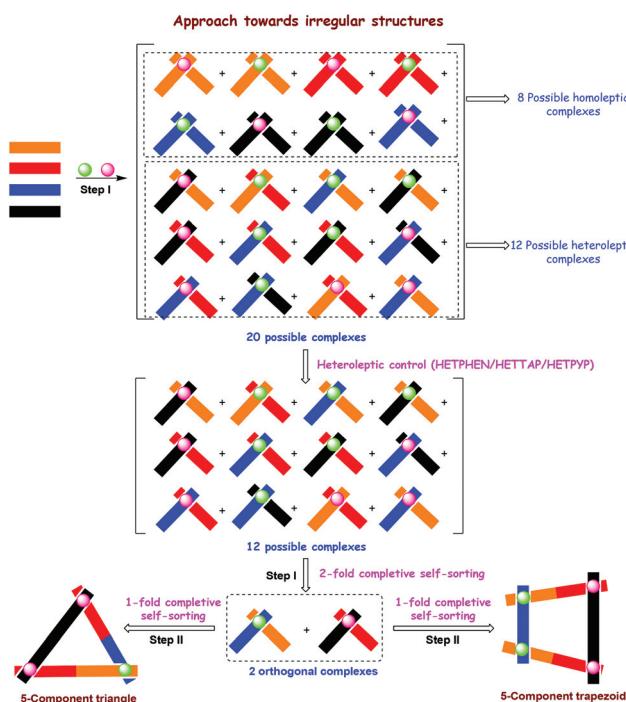


Fig. 4 Cartoon representation of 2-fold compleptive and 1-fold compleptive self-sorting processes.

dynamic heteroleptic binding motifs in such a way that they remain *orthogonal*<sup>20</sup> despite the fact that all motifs can easily undergo ligand and/or metal exchange reactions. Clearly, the required constitutional selectivity itself is not implemented in our heteroleptic toolkits (*vide supra*), as they are programmed

at preventing the formation of homoleptic complexes, but at the onset do not provide the means of differentiating between various alternative heteroleptic combinations (Fig. 4). To address the latter issue, we probed *x*-fold *compleptive* self-sorting in a library of mononuclear cornerstones (Fig. 4, step I) until we were able to identify heteroleptic complexes that formed without interference. These motifs were later merged in multiligand building blocks for *integrative* (= *1-fold compleptive*) self-sorting<sup>49</sup> thus precluding any undesired side products (Fig. 4, step II). Undoubtedly, even in such an approach each individual component needs to be carefully instructed in such a way that sophisticated recognition patterns identify correct combinations while rejecting wrong arrangements.

Our methodology allows one to selectively fabricate geometrically and compositionally *irregular* supramolecules (Fig. 4) as a single species from a pool of *communicative* ligands and metal ions.<sup>20</sup> Clearly, in the exemplarily shown triangle and trapezoid the diversity and complexity are largely increased in contrast to those of our previous oligonuclear three-component structures (chapter 2), because the latter are only based on one type of heteroleptic algorithm, *e.g.* either HETPHEN, HETTAP or HETPYP. Based on this strategy we are able to prepare metallocycles that utilise five to seven different components in their framework (*vide infra*, Schemes 5–7). However, to our appreciation, the approach as outlined in Fig. 4 holds promise for even larger dynamic structures encompassing more than seven components in the near future, quite a significant advancement in a field long dominated by two- or three-component structures.<sup>22b</sup> In the following, we will portray some of our recent examples by classifying them along an increasing number of heteroleptic algorithms.

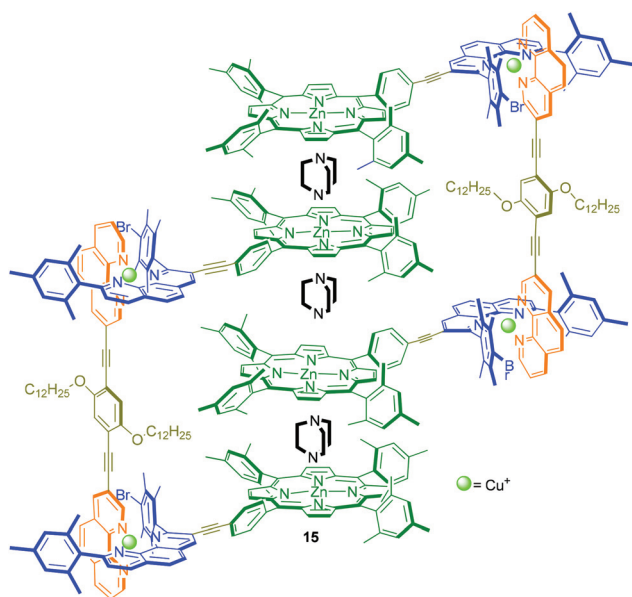


Fig. 5 Four-component porphyrins stack **15**.<sup>32</sup>

### 3.1. Amalgamation of two heteroleptic motifs

**Merging HETPHEN and *N*→zinc(II) porphyrin complexation.** In 2006, by demonstrating orthogonality between the HETPHEN and the well-known *N*→zinc(II) porphyrin coordination, we accomplished our first example of a 2-fold completable self-sorting.<sup>28b,32,50</sup> The 2-fold self-sorting algorithm was highly useful to quantitatively prepare dynamic three-component heterometallic rectangles,<sup>28b</sup> four-component discrete porphyrin stacks such as **15** (Fig. 5),<sup>32</sup> and a fullerene-porphyrin-Cu(phen)<sub>2</sub>-ferrocene tetrad.<sup>50</sup> Notably, all structures are accessible by mixing the different components in any sequence as long as the stoichiometry is obeyed.

**Merging HETPHEN and HETTAP complexation.** Lately, in 2009, we developed a 2-fold completable self-sorting<sup>22c</sup> process furnishing the HETPHEN and HETTAP complexes **20** and **21** in an interference-free manner (Scheme 5a).<sup>51</sup> Considering the stability of other possible HETPHEN and HETTAP complexes, one expects at least the formation of four complexes, *i.e.*, **20–23**, from an equimolar mixture of ligands **16–19**, Zn<sup>2+</sup> and Cu<sup>+</sup> ions. To our understanding, the observed selectivity toward **20** and **21** is guided by the correct stoichiometry, precise tuning of steric and electronic effects, π–π interactions, and metal-ion coordination specifics. With reference to copious reported complexes, we<sup>52</sup> and others have stated that a Cu<sup>+</sup> ion as a rule will be tetrahedrally coordinated by four donor atoms only – even if the surrounding ligands provide more than four. In contrast, Zn<sup>2+</sup> has the ability to vary and expand its coordination number while preferring an octahedral geometry.<sup>37</sup> Based on this fact, we reasoned that the additional Zn···OMe ion-dipole interaction(s) present in **21** would provide a suitable *pseudo*-octahedral geometry to the Zn<sup>2+</sup> ions thus enthalpically (log β ≈ 14) supporting its formation while disfavouring the alternative HETTAP complex **23**

(log β ≈ 12). At the accurate stoichiometry, the Zn<sup>2+</sup> ions will make full use of ligands **17** & **18** to afford **21** and thus drive the formation of **20** *via* maximum site occupancy and HETPHEN control. Interestingly, in a control experiment an equimolar mixture of ligands **16**, **17**, **19** and Cu<sup>+</sup> ions did not contain the needed information to bias formation of **20** over that of **22**, but instead produced a jumble of **20**, **22** and free ligands **16**, **17**. To our appreciation, complex **21** thus behaves as a *molecular chaperone* that guides the 2-fold completable self-sorting process (Scheme 5a).

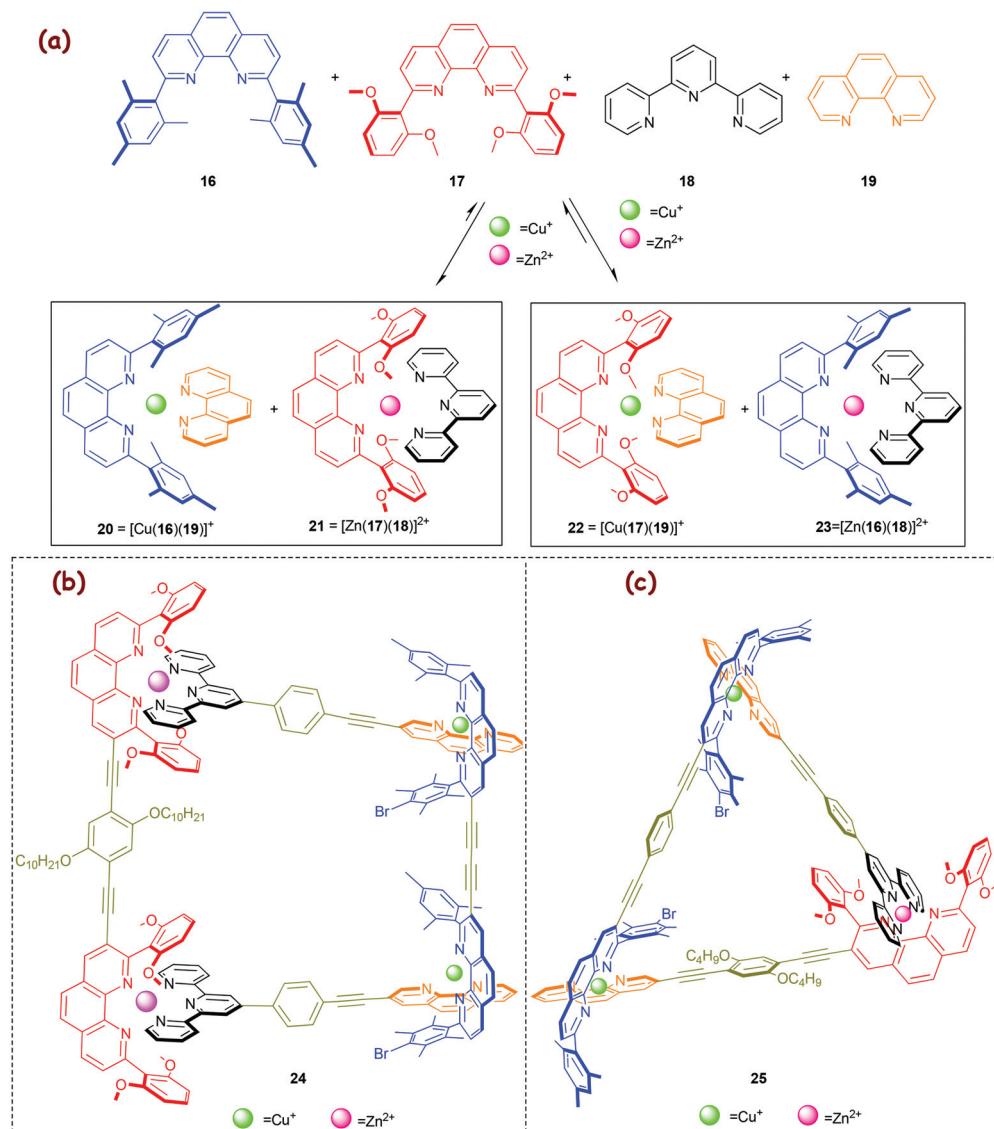
The above 2-fold completable self-sorting protocol was first challenged in the fabrication of the five-component isosceles trapezoid **24** (Scheme 5b).<sup>51</sup> Later, the same motifs were applied to construct the five-component triangle **25** (Scheme 5c).<sup>53,54</sup>

**Merging HETPHEN and HETPYP-I complexation.** In 2013, we capitalised on the aforementioned *molecular chaperone* **21** (Scheme 5) to direct a much more demanding self-sorting scenario toward the *valence frustrated* tri-coordinated HETPYP-I copper(I) complex **27** = [Cu(**16**(**26**)](PF<sub>6</sub>) (log β ≈ 8) that is depicted in Scheme 6.<sup>55</sup> To our delight, the higher stability of complex **21** (Δlog β ≈ 2) compared to that of the alternative complex **23** (Scheme 5a) is sufficient to drive the much weaker HETPYP-I complex **27** based on thermodynamic preferences.<sup>56</sup> In a follow-up 1-fold *completable* self-sorting we efficaciously used both orthogonal motifs for the clean preparation of the five-component trapezoid **28** and triangle **29**, with the weakly binding HETPYP-I motif contributing to 2 out of 4 (in **28**) or 3 (in **29**) cornerstones (Scheme 6). A comparison of trapezoids **24** (Scheme 5) and **28** (Scheme 6) reveals that the use of the C<sub>s</sub>-symmetric HETPYP-I complex units in **28** avoids the formation of diastereomeric structures, thus greatly facilitating its characterisation *via* <sup>1</sup>H NMR.

### 3.2. Merging HETPHEN, HETTAP and *N*→zinc(II) porphyrin complexation

In 2010, a new eight-component library (Scheme 7a)<sup>57</sup> was elaborated from the earlier six-component library (Scheme 5a), by juxtaposing the pyridine→zinc porphyrin coordination (log K ≈ 3.0–3.7) aside of the HETPHEN and HETTAP motifs. Orthogonality of the pyridine→zinc porphyrin motif **31** = [(**26**) (**30**)] with our heteroleptic complexes is readily implemented due to the optimal saturation of all ligands and metal ions in complexes **20**, **21** and **31**. Moreover, it is supported by the inability of the bi- or tridentate ligands **16–19** to interact with zinc porphyrin **30** due to high steric shielding. Noticeably, in the present library (Scheme 7a) only three of 35 possible complexes do form (3-fold completable self-sorting), while from our original library (Scheme 5) two complexes emerged out of twenty different combinations. Because detrimental *cross-talk* in general rapidly increases with an augmenting number of components,<sup>20</sup> a more sophisticated *molecular programming* is required for any larger self-sorted library.<sup>49</sup>

We exploited the three orthogonal complexes as three cornerstones in the scalene triangle **32** (Scheme 7b). Because Hg<sup>2+</sup> ions form stronger HETTAP complexes than Zn<sup>2+</sup> (Δlog



**Scheme 5** (a) Merging HETPHEN and HETTAP approaches in a 2-fold compleptive self-sorting process.<sup>51</sup> Five-component supramolecular (b) trapezoid 24<sup>51</sup> and (c) triangle 25<sup>53</sup> fabricated from 1-fold compleptive self-sorting.

$\beta \approx 2$ ,<sup>36</sup> addition of one equivalent of Hg<sup>2+</sup> to 32 caused a metal displacement furnishing 33. To the best of our knowledge, 33 is the first trisheterometallic supramolecular scalene triangle with three different self-assembled corners.<sup>57</sup>

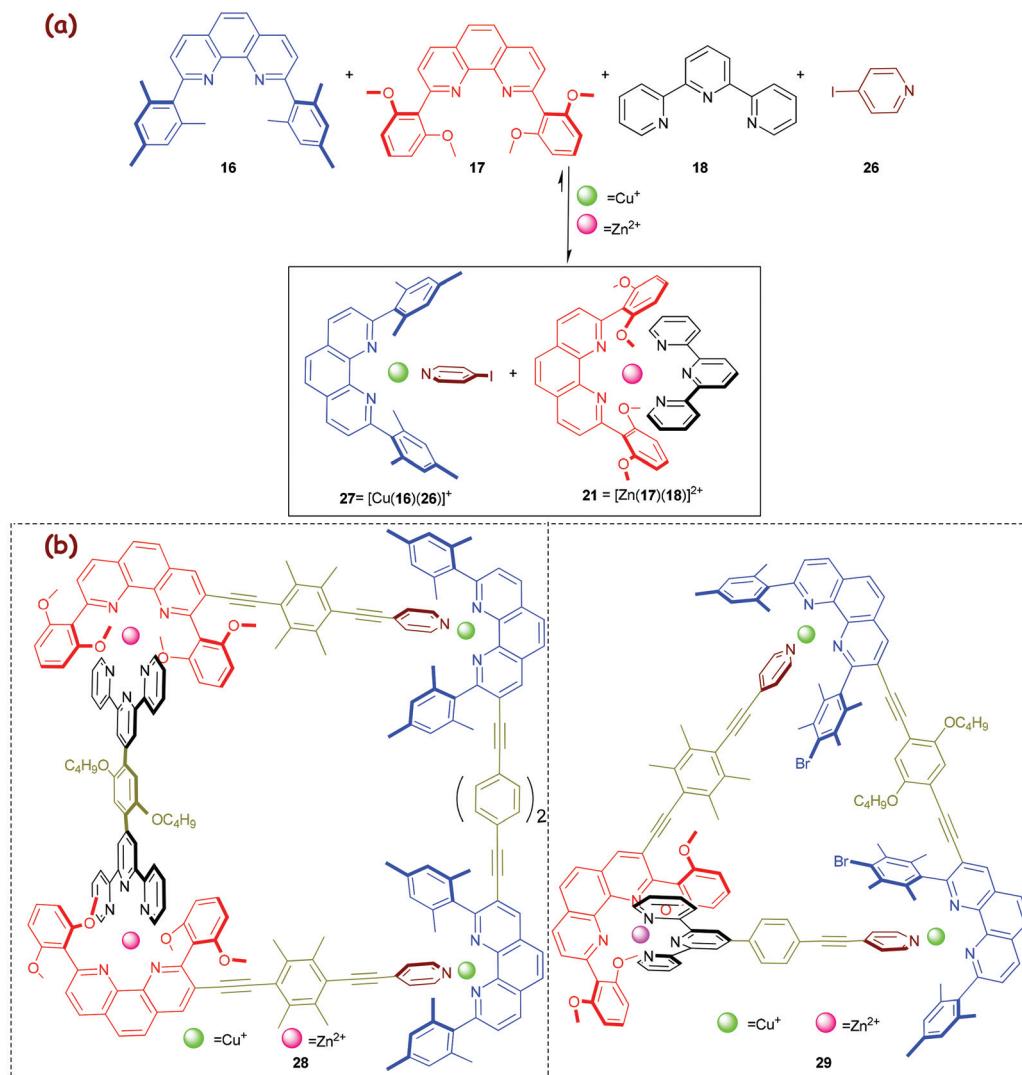
Very recently, we used the insight on constitutionally dynamic heteroleptic  $[\text{M}(\text{phen}_{\text{Ar}2})(\text{iminopyridine})]^{n+}$  complexes (Fig. 3 and Scheme 3b) in a 3-fold compleptive self-sorting as described in Scheme 7a for the fabrication of the scalene quadrilateral 34 that encompasses seven distinct components in its framework (Scheme 7c).<sup>37</sup> To the best of our knowledge the quadrilateral represents the *state-of-art* in self-sorting of supramolecular entities, as the degree of self-sorting is much higher than that in any other case reported so far.

Summing up section 3, clearly the amalgamation of multiple similar and archetypically different interactions has been successful to access multicomponent structures of much

higher complexity and diversity. Considering the present level of self-sorting, the scene is set for devising novel functional properties that emerge from spatial and electronic specifics in multicomponent aggregates.

## 4. Functions and applications

Implementation of emergent functions in multicomponent assemblies is currently one of the major challenges. Because any emergence arises only when all components find themselves in the proper spatiotemporal arrangement, it may not be directly predicted by considering the subcomponents in isolation.<sup>58,59</sup> To this end, our heteroleptic toolkits with their high level of constitutional control in combination with self-sorting (*vide supra*) offers new chances for the rational design



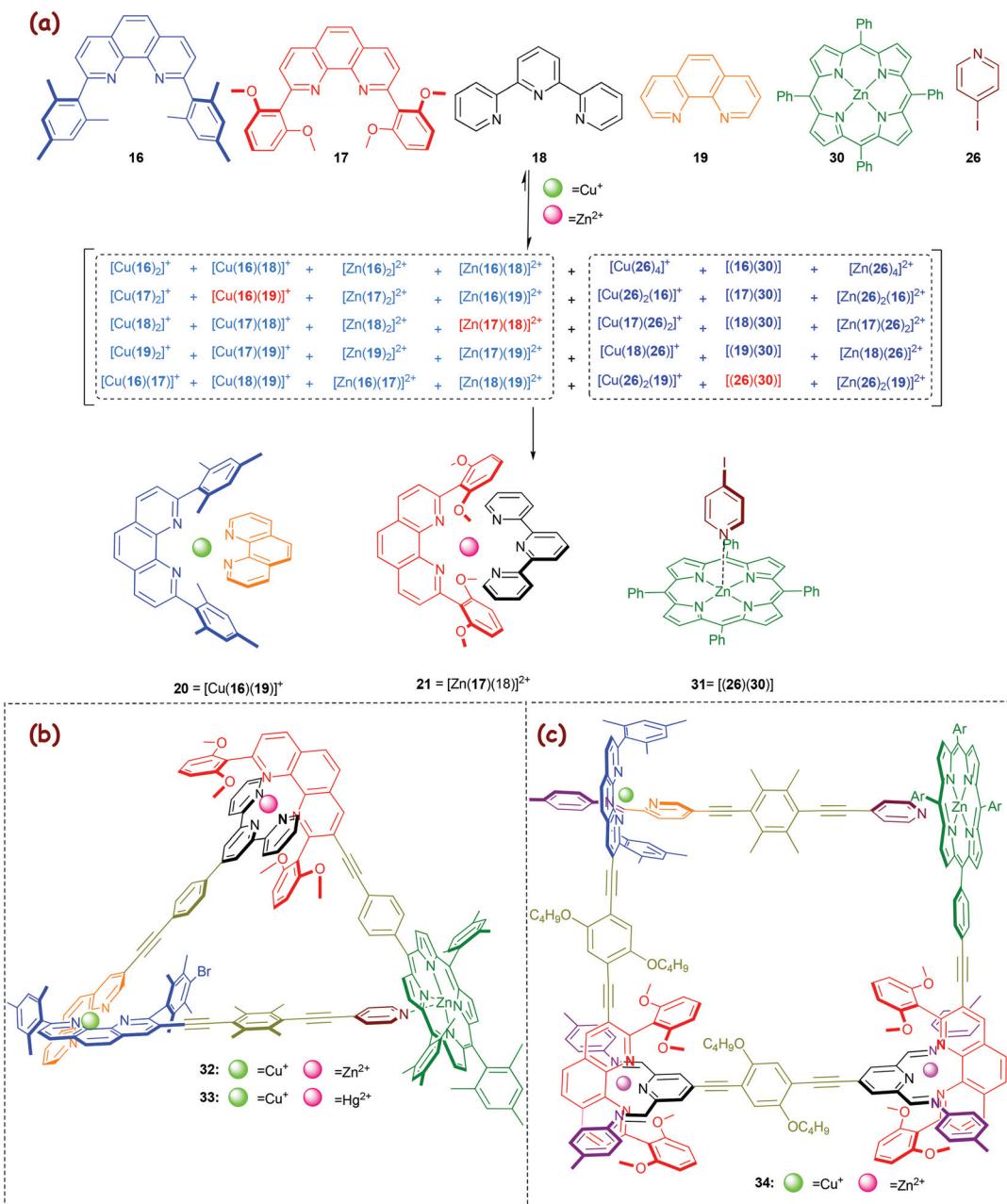
**Scheme 6** (a) Exclusive formation of the weakly linked HETPYP-I complex **27** and the strongly associated HETTAP complex **21** from a 6-component library. (b) Chemical structures of the five-component supramolecular isosceles trapezoid **28** and triangle **29**.<sup>55</sup>

of multicomponent assemblies with tunable properties, as guided by compositional, constitutional and conformational changes. In recent years, our research has thus shifted toward functional nano-assemblies in various areas, as diverse as supramolecular splicing,<sup>60</sup> metal ions sensing,<sup>38</sup> nano-switches,<sup>61</sup> molecular electronics,<sup>62</sup> host-guest chemistry,<sup>63</sup> dynamic polymers,<sup>34c</sup> etc. In addition, our heteroleptic toolkits have served other groups<sup>64-67</sup> to build nanorotors and solar cells among others. In the ensuing section, we will portray some of our recent systems that have already exhibited promising potential for future applications.

#### 4.1. Guest adaptive frameworks

Over the past two decades, 3D metallocsupramolecular hollow complexes of well-defined shapes and sizes have received frequent attention in the context of fascinating host-guest chemistry, as evidenced by impressive examples by Stang,<sup>7</sup> Fujita,<sup>46</sup> Raymond,<sup>46</sup> Nitschke,<sup>4</sup> Clever<sup>68</sup> and many others.<sup>59</sup> Recent

highlights even include modulation of guest reactivity, cavity-controlled catalysis, gas storage, separation, etc. Quite often, such complex structures provide an adaptable cavity size that allows encapsulation of different guests in a regulated manner. Along this line, we described in 2008 how added guests regulate the shape of a supramolecular three-component assembly (Scheme 8) by providing either the nanoprism **39** = **38**@**37** or the constricted nanoframework **40** = **C**<sub>60</sub>@**37**.<sup>69</sup> Explicitly, the desired nanoprism **37** =  $[\text{Cu}_6(35)_2(36)_3]^{6+}$  is not exclusively assembled from its precursors without the strong supramolecular assistance from either **38** or **C**<sub>60</sub>, most likely due to the thermodynamically competitive formation of some small oligomeric aggregates. Clearly, the strong binding and good spatial match between the three pyridine nitrogens of **38** and the three zinc porphyrin units in **37** is the key to convert the dynamic mixture into a single species **39**. The role of **C**<sub>60</sub> is more remarkable as it forces **37** to adapt a smaller cavity size in order to maximise the



**Scheme 7** (a) 3-Fold completable self-sorting in an eight-component library. (b) Chemical structure of the scalene triangles **32–33**<sup>57</sup> and (c) the scalene quadrilateral **34**.

porphyrin–fullerene interactions, affording an accordion-type host–guest system that wraps around  $\text{C}_{60}$ , as demonstrated in Scheme 8.

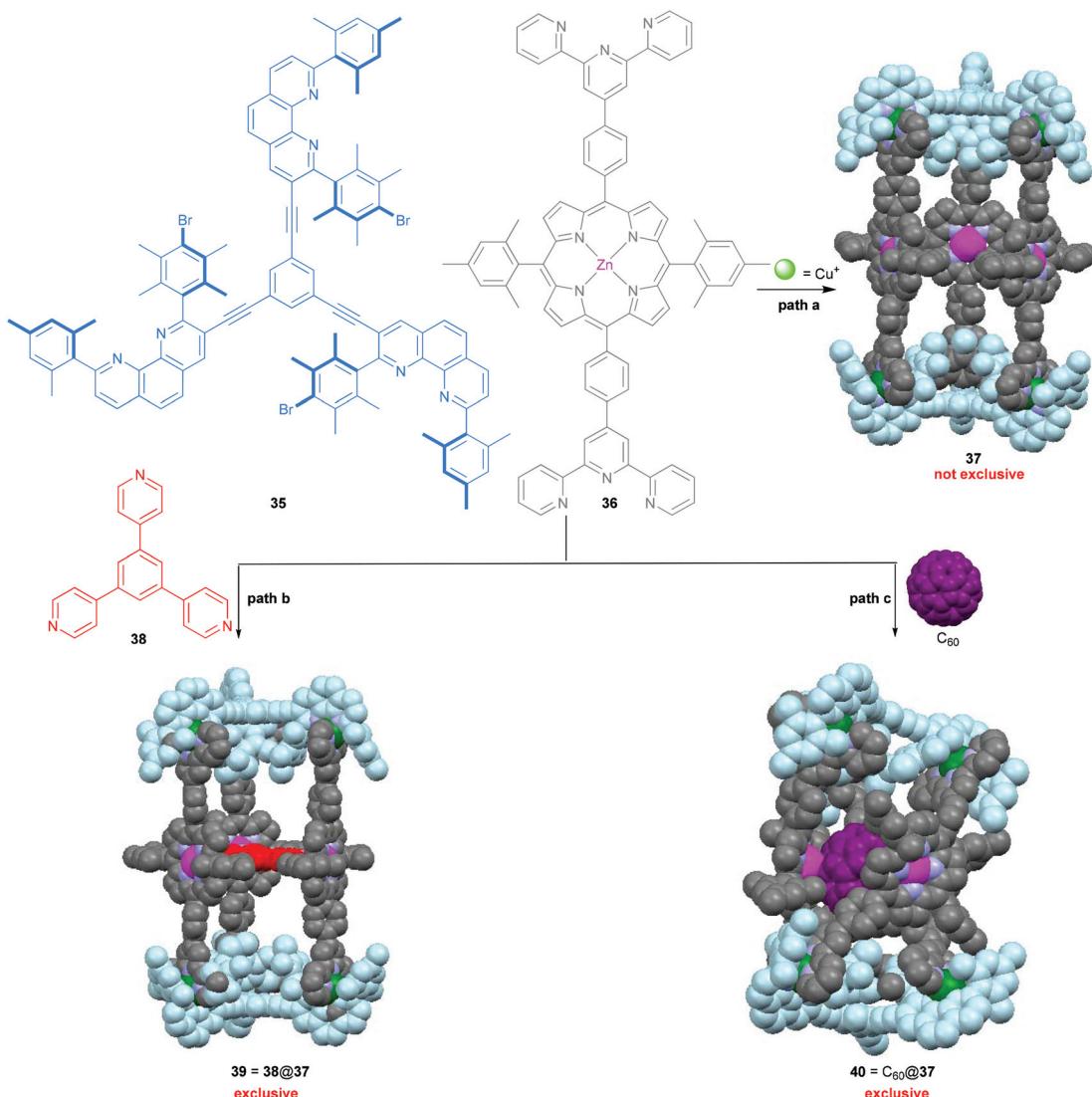
Lately, using the  $[\text{Cu}(\text{phen}_{\text{Ar}2})(\text{picolinaldehyde})]^+$  complexation motif, we fabricated a heteroleptic 3D metallosupramolecular tetragonal prism that behaves as a flexible and guest-adaptive host encapsulating either  $\text{C}_{60}$  or coronene.<sup>63</sup>

#### 4.2. Metal exchange and fluorescence signalling

The diverse luminescence properties of polynuclear  $d^{10}$  metal complexes have found ample application.<sup>70</sup> Our efforts in this area focused on a  $\text{Cu}^{2+} \rightarrow \text{Zn}^{2+} \rightarrow \text{Hg}^{2+}$  transmetalation<sup>71</sup> in a

HETTAP nanoladder assembly that was readily recognised by the naked eye, as zinc(II) ladders have strong emissions in contrast to their copper(I) and mercury(II) analogues (Fig. 6).<sup>36</sup> The protocol is easily understood considering the association constants that vary substantially for HETTAP complexes along the series:  $\log \beta \approx 9.3$  ( $\text{Cu}^{2+}$ ), 12.4 ( $\text{Zn}^{2+}$ ) and 14.7 ( $\text{Hg}^{2+}$ ). As a result, the transmetalation ( $\text{Cu}^{2+} \rightarrow \text{Zn}^{2+} \rightarrow \text{Hg}^{2+}$ ) resulted in an *OFF*→*ON*→*OFF* emission response.

Capitalising on the above insight, we realised chemosensing with the zinc(II) based HETTAP clip **47** (Scheme 9),<sup>38</sup> containing an oligoether unit at the periphery for metal cation recognition. Indeed, within the small series of cations ( $\text{Na}^+$ ,



Scheme 8 Synthesis of the shape-adaptive nanoprism **37** =  $[\text{Cu}_6(35)_2(36)_3]^{6+}$ <sup>69</sup>

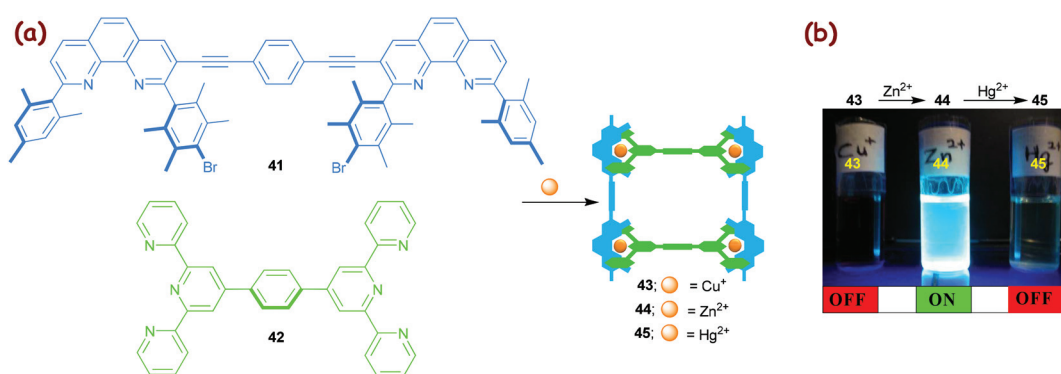
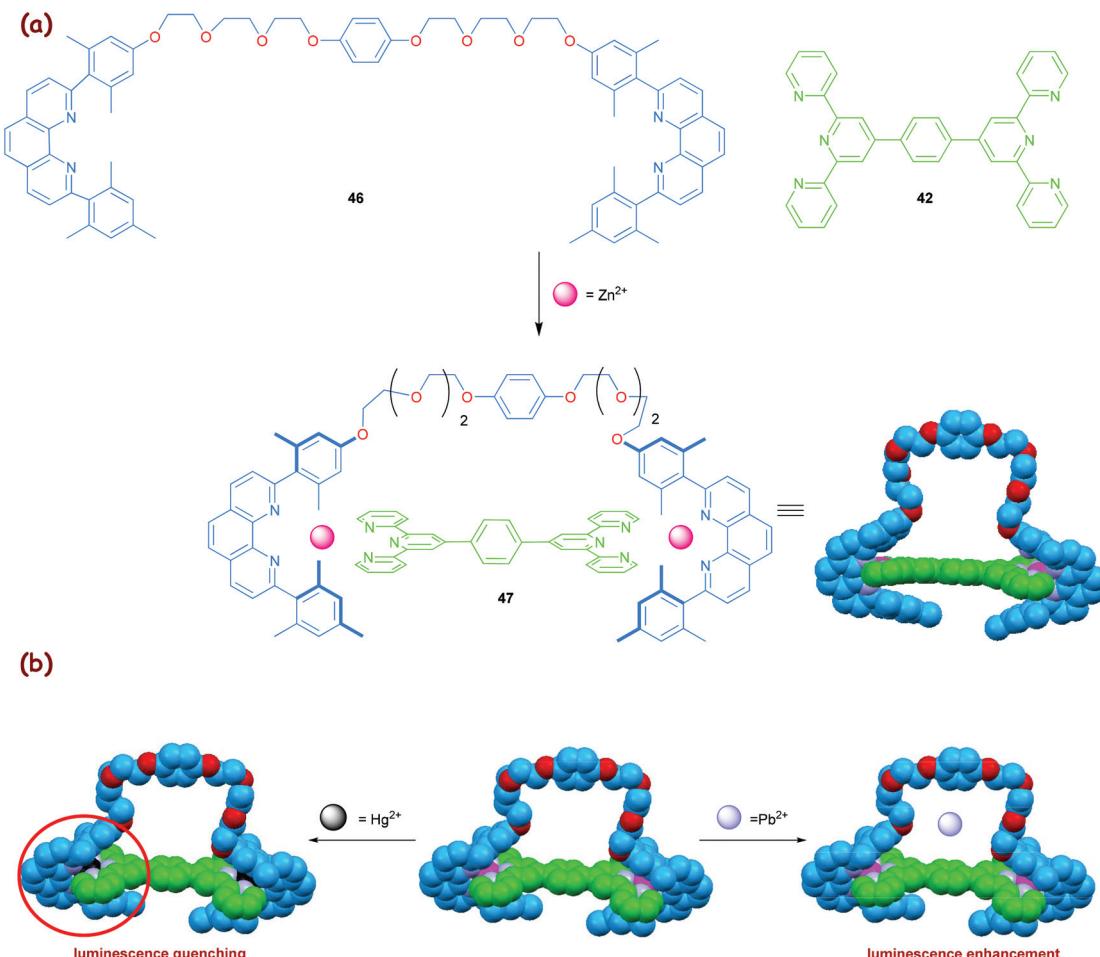


Fig. 6 (a) Synthesis of the three-component HETTAP ladders **43–45**. (b) A two-step transmetalation OFF→ON→OFF fluorescence cascade. The zinc(II) ladder **44** shows a strong emission at  $\lambda_{\text{em}} = 463 \text{ nm}$  ( $\lambda_{\text{ex}} = 389 \text{ nm}$ ).<sup>36</sup> The artwork in (b) is reprinted from ref. 36 with the permission of the American Chemical Society (Copyright 2005).



Scheme 9 (a) Synthesis of clip 47 and (b) its metal ions sensing by a luminescence probe.<sup>38</sup>

$K^+$ ,  $Mg^{2+}$ ,  $Ca^{2+}$ ,  $Pb^{2+}$  and  $Ba^{2+}$ ), the strongest luminescence increase was found upon addition of  $Pb^{2+}$  ions (50% enhancement with respect to 47). In contrast,  $Hg^{2+}$  behaves ambivalently, as the luminescence strongly depends on its relative amount. Upon substoichiometric addition, the luminescence intensity of clip 47 was first increased ( $\sim 20\%$  to 30%) but then became constant upon addition of just 1 equiv. of  $Hg^{2+}$ . Further addition of  $Hg^{2+}$  efficiently quenched the luminescence. To our understanding, the increase of the luminescence may be assigned to an association of the metal ions with the oligoether tether of 47 (Scheme 9b). A second mechanism operates for  $Hg^{2+}$  at higher concentration. The decrease in luminescence is due to a  $Zn^{2+} \rightarrow Hg^{2+}$  exchange process in 47, analogous to that in Fig. 6b, which leads to quenching. The clip 47 thus exhibits a highly selective response toward  $Hg^{2+}$  due to supramolecular effects.

#### 4.3. Supramolecular fusion

Stimuli-triggered supramolecular rearrangements have attracted continued attention due to their critical importance in both biological systems<sup>72</sup> and toward the preparation of sophisticated molecular machines and switches<sup>73</sup> (*vide infra*).

At present, the current generation of switchable assemblies mainly involves two-state self-assembled aggregates, where the connectivity patterns are altered by switching molecular binding properties through chemical, photochemical or electrochemical inputs. In this *modus operandi*, self-assemblies are quite often either disassembled upon stimulation (e.g., pseudorotaxanes and tetrahedra) or only toggled within the same architectural manifold.<sup>74</sup> In contrast, Nature elegantly uses *gene shuffling*, *i.e.* combination of dissimilar genes, to produce new emergent genes.<sup>75</sup> To our understanding, as the original supramolecules already represent some chemical information, the implementation of an analogous supramolecular transformation may result in an *evolution* toward higher information content. For example, consider a simple case where two square architectures are fused into a rectangle, *i.e.*  $S1 + S2 \rightarrow R1$  (Fig. 7). The precursor squares are fully defined by the length of one side, while the description of the rectangle requires two pieces of information, *i.e.* two different lengths. Clearly, in such processes the diversity and complexity will be increased by enlarging the number of different components.

To this end, initial *proof-of-concept* experiments in our laboratories established the fabrication of the 5-component

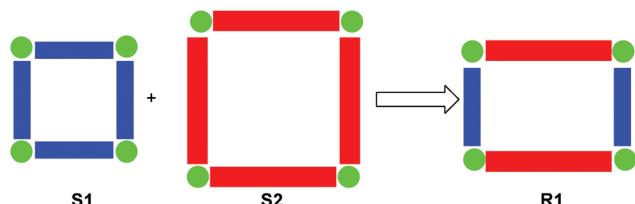
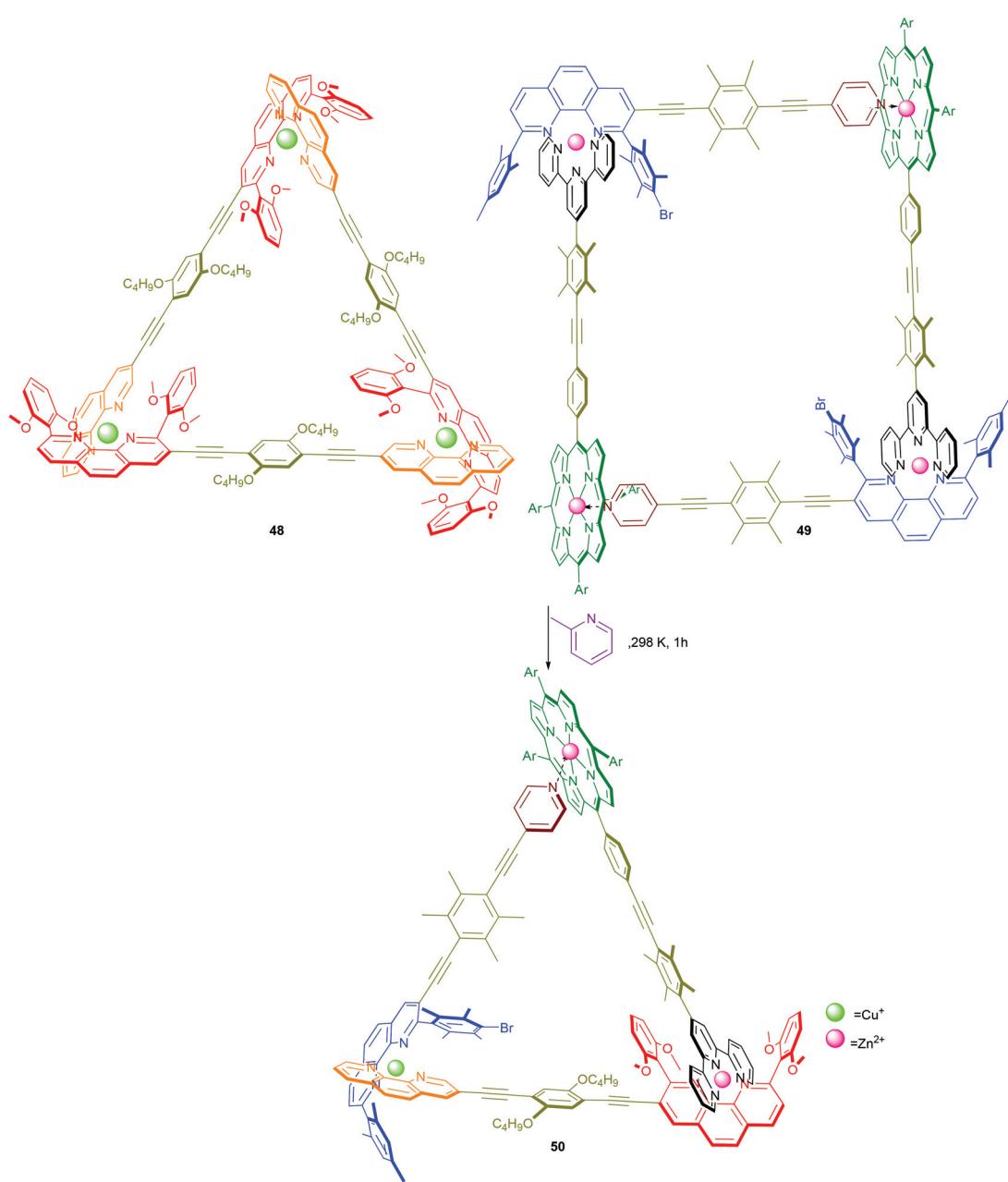


Fig. 7 Cartoon representation of a supramolecular fusion.

scalene triangle **50** by a spontaneous or catalytic supramolecular fusion of two distinct and dynamic supramolecules, namely equilateral triangle **48** and rectangle **49** (Scheme 10).<sup>60</sup>

Because the metal corners are thermodynamically less favoured in both **48** and **49** (Scheme 7), upon mixing the components re-shuffle to form the more favourable assembly **50**. Whilst the spontaneous process takes 15 h at room temperature, the transformation is completed within 1 h in the presence of catalytic amounts of 2-methylpyridine. To our evaluation, the latter transformation comprises several distinct chemical events, including (i) favoured pair-selection due to a high fidelity *3-fold compleutive self-sorting* (Scheme 7); (ii) *error-correction* under thermodynamic control; and (iii) acceleration of a supramolecular fusion reaction *via* labilisation of the metal-ligand bonds.



Scheme 10 Catalytic fusion of **48** and **49** to **50**.<sup>60</sup>

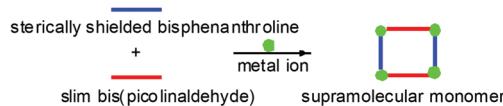


#### 4.4. Multiple-stranded dynamers

With the growing interest in functional supramolecular materials, the *art of dynamer synthesis*<sup>6</sup> has become an escalating field of research in the last two decades. Consequently, many effective synthetic approaches have been developed that provide easy access to single-stranded dynamers.<sup>76</sup> In contrast, multiple-stranded dynamers are hitherto extremely rare because of preparative problems as well as serious characterisation difficulties. With the aim of developing a ready-to-use synthetic methodology for multiple-stranded dynamers we recently developed the *Template Directed Constitutional Dynamic Polymerisation* (TD-CDP) approach<sup>34c</sup> (Fig. 8) based on constitutional dynamic chemistry and heteroleptic aggregation (Fig. 3). In Fig. 8, the full process is depicted in a pictorial manner for a difunctional supramolecular template.

To illustrate the conceptual idea in a schematic manner, consider HETPHEN-based supramolecular aggregates (Step 1) that may act as sophisticated “monomeric units” in the TD-CDP. With their reactive aldehyde terminals they are perfectly suited for constitutionally dynamic polyimine formation in the

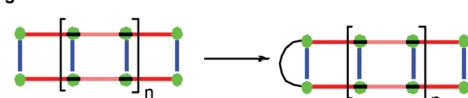
#### Step 1: HETPHEN regulated supramolecular monomer synthesis



#### Step 2: Correlated growth in polyimine strands



#### Step 3: End capping



#### Step 4: Post polymerisation treatment

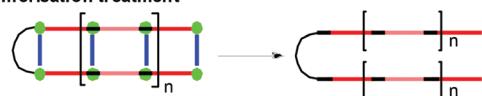
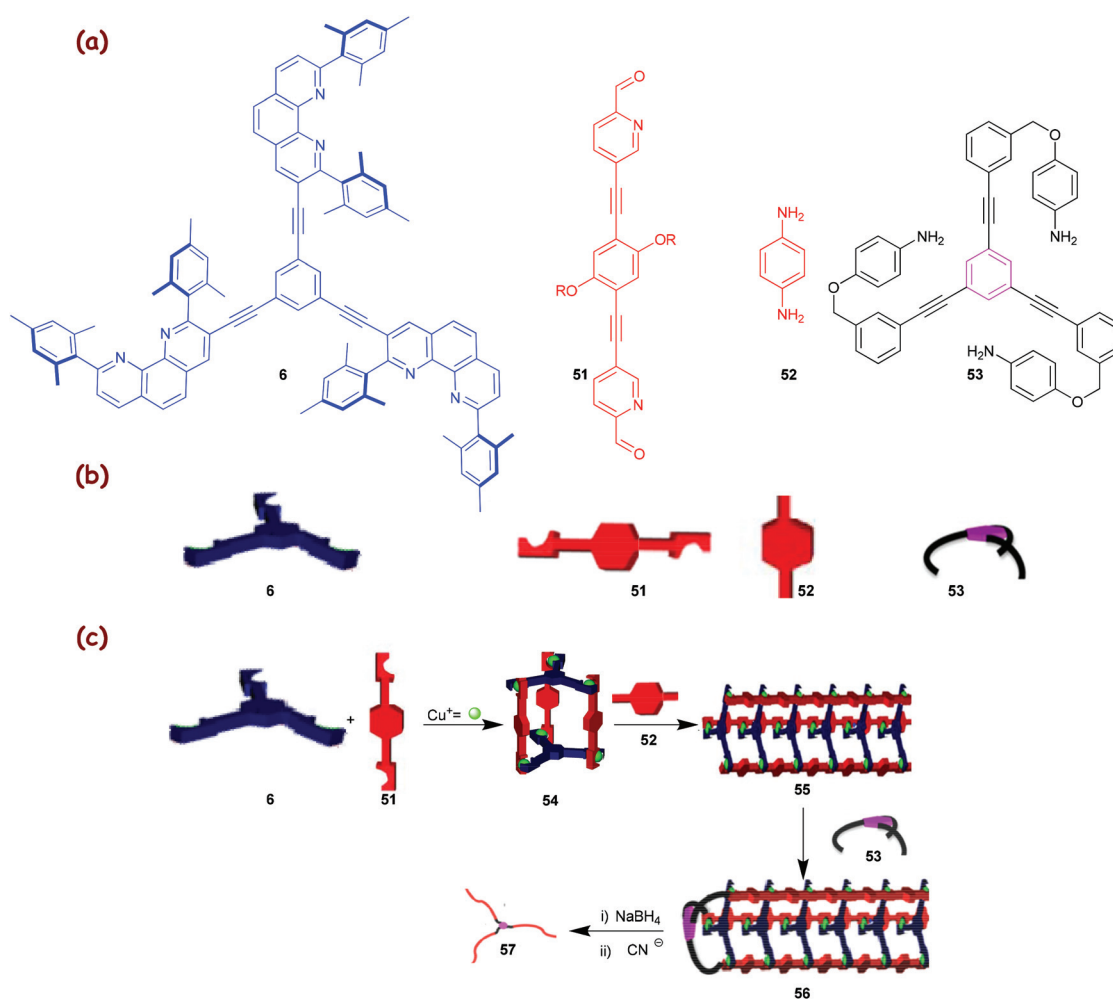


Fig. 8 Cartoon representation of the TD-CDP approach for a difunctional supramolecular template.



**Scheme 11** (a) Chemical structures of ligands 6 and 51–53; (b) their cartoon representations; (c) the TD-CDP approach with a trigonal nanocage 54.<sup>34c</sup> The artwork in Scheme 11 is reprinted from ref. 34c with the permission of the American Chemical Society (Copyright 2012).



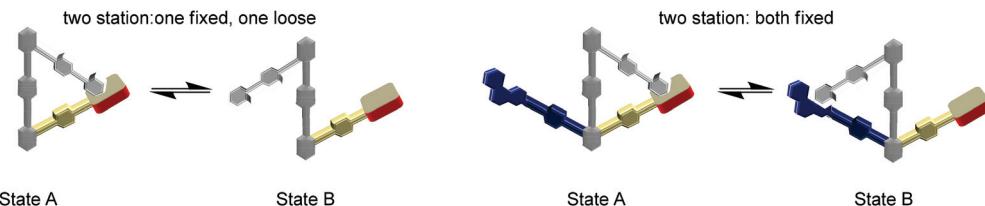


Fig. 9 Development of new rotary nanoswitches.

presence of suitable diamines (step 2). Most importantly, the polymerisation step intrinsically bears the promise for effective control of the parallel growth of two, three or even more polymer strands, as all strands are expected to grow at the same pace. The metal phenanthrolines have a triple role. They act as a *supramolecular template*, catalyse the reversible iminopyridine formation and finally bind them as ligands thus setting up two, three or more parallelly growing polymer strands. For example, elongation at any arbitrary strand, *e.g.* 'strand one', will preorganise the template such that the second and following strands will profit from cooperative effects in their elongation step. Hence, due to the dynamic heteroleptic coordination at the terminus of the growing polymer, a template with  $n$  phenanthroline sites will support parallel growth of  $n$  polymer strands in high fidelity. Finally, to evaluate the correlated growth of strands in multi-stranded polymers, end capping at one end of the multi-stranded dynamer (step 3) followed by a reductive post-polymerisation treatment of the resulting dynamic polymer (step 4) was required to kinetically lock and liberate the polymer from the supramolecular scaffold.

The principle, laid out in Fig. 8, opens many options for the preparation of compounds and materials with uncommon topology, such as supramolecular nanoscale cocoons, ribbons and filaments or polymers with a high constitutional fidelity. The methodology should also allow the preparation of bicyclic, polycyclic and star polymers with identical lengths of all strands, with the prospect that these yet unknown polymeric materials may convey interesting properties. In a recent communication, we demonstrated the usefulness of our concept developing dynamer 55 (Scheme 11) with three strands and its transformation into the covalent star polymer 57 that has arms of similar length ( $\sim 72\%$ ) as demonstrated by AFM.<sup>34c</sup>

#### 4.5. Novel nanoswitches

There is no life without *molecular switching*, as it plays a crucial role in almost all aspects of our existence.<sup>77</sup> For example, many important biological machines (F1-ATPase, kinesin, RNA polymerase, helicases, *etc.*) rely on immense structural changes as a basis for their action. The structural changes actually provide the required electronic and steric alterations in the *active site* that empower the desired action. Thus, all machines must receive clear ON/OFF signals from the signalling network of the organism to control their action.<sup>78</sup> Over the years, the *modus operandi* of the biological

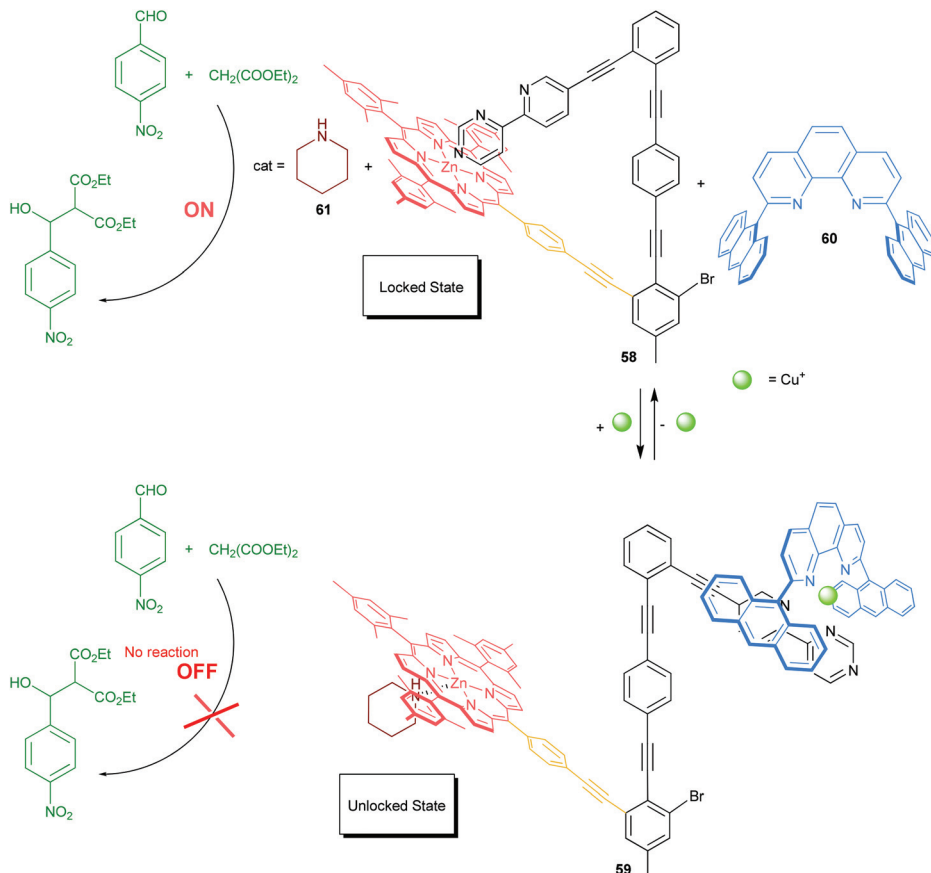
machinery has been serving as a constant source of inspiration for the design of prototypical artificial switches and machines, with the goal to mimic at least some part of the biological complexity. Our endeavours in this direction have led to two-stage rotary nanoswitches with a triangular architecture (Fig. 9) that can be reversibly and repeatedly toggled to control a chemical reaction in an ON and OFF manner.<sup>61</sup>

In 2012, we reported on the chemically triggered self-locking nanoswitch 58 and its reversible locking and unlocking, which mimics in part the working principle of CaMKII (Scheme 12).<sup>61a</sup> To serve the purpose, we implemented a sophisticated azabipyridine unit into the nanomechanical arm that may engage in the formation of either a pyridine $\rightarrow$ zinc(II) porphyrin motif (*locked state*) or HETPEN-like  $[\text{Cu}(\text{phenanthroline})(\text{bipyridine})]^+$  motif (*unlocked state*). Originally, the nanoswitch 58 is locked at the azabipyridine $\rightarrow$ zinc(II) porphyrin linkage, but switching is possible by addition or removal of  $[\text{Cu}(60)]^+$  ions. The switching of 58 was exploited to reversibly toggle ON-OFF an organocatalytic Knoevenagel addition. As depicted in Scheme 12, in the ON state, the strong intramolecular association at the pyridine $\rightarrow$ zinc(II) porphyrin linkage prevents piperidine (61) from binding to the zinc(II)-porphyrin unit of the switch. Addition of  $[\text{Cu}(60)]^+$  ions as an input signal generates the heteroleptic complex 59 =  $[\text{Cu}(58)(60)(61)]^+$  liberating the arm from the zinc porphyrin station in 58. The liberated zinc porphyrin binds strongly to piperidine (61) preventing its function as an organocatalyst. Lately, we refined the approach by merging the shielded phenanthroline unit into the switch. The modified switch acts as a photocatalyst for the isomerisation of diazastilbene.<sup>61b</sup>

#### 4.6. Novel supramolecular nanorotors

The rational design and synthesis of multicomponent supramolecular machines constitute a fascinating challenge in the field of nanoscience.<sup>5</sup> Indeed, a huge majority of reports cover covalent machines, while fully dynamic and artificial supramolecular devices, like Stoddart's supramolecular valves,<sup>79a</sup> Aida's nanomechanical tweezers<sup>79b</sup> or Shionoya's double-ball bearing complexes,<sup>79c</sup> constitute rare examples in a wide *terra incognita*. Adding to the latter field, we recently elaborated a family of four-component supramolecular nanorotors that undergo fast ( $\geq 78\,000\text{ s}^{-1}$ ) stochastic rotary oscillations at 298 K (Scheme 13) but that are virtually stopped ( $\leq 18\text{ s}^{-1}$ ) at 198 K.<sup>80</sup> Remarkably, both kinetic and thermodynamic data suggest the spinning motion in the rotors to take place solely by an





Scheme 12 Organocatalysis toggled ON/OFF with nanoswitch 58.<sup>61a</sup>

intrinsupramolecular pathway (>99.9%) despite operating across a dynamic hinge. For instance, the nanorotor 64 (Scheme 13) was designed based on two orthogonal coordination motifs, *i.e.* a HETPYP-I type and a DABCO $\rightarrow$ zinc(II) porphyrin complexation. Reacting the two different zinc(II) porphyrins 62 & 63, DABCO as a dynamic hinge and copper(I) ions in a ratio of 1:1:1:2 furnished quantitatively the self-assembled nanorotor 64 with platform 62 representing the stator and 63 the rotator. To our understanding, the two HETPYP-I units in 64 actually ensure and guide the formation of the DABCO-bis(porphyrin) hetero-sandwich. In nanorotor 64, the rotator 63 is spinning across the dynamic axle in 180° steps, while upon feeding the unloaded phenanthroline stations with Cu<sup>+</sup> ions thus generating nanorotor 65, the oscillating rotation will proceed *via* mixed 90°/180° steps. A kinetic analysis reveals that depending on the mode of rotation the speed of the spinning motion is different and that speed regulation is thus possible through a reversible 64  $\rightleftharpoons$  65 nanorotor transformation.

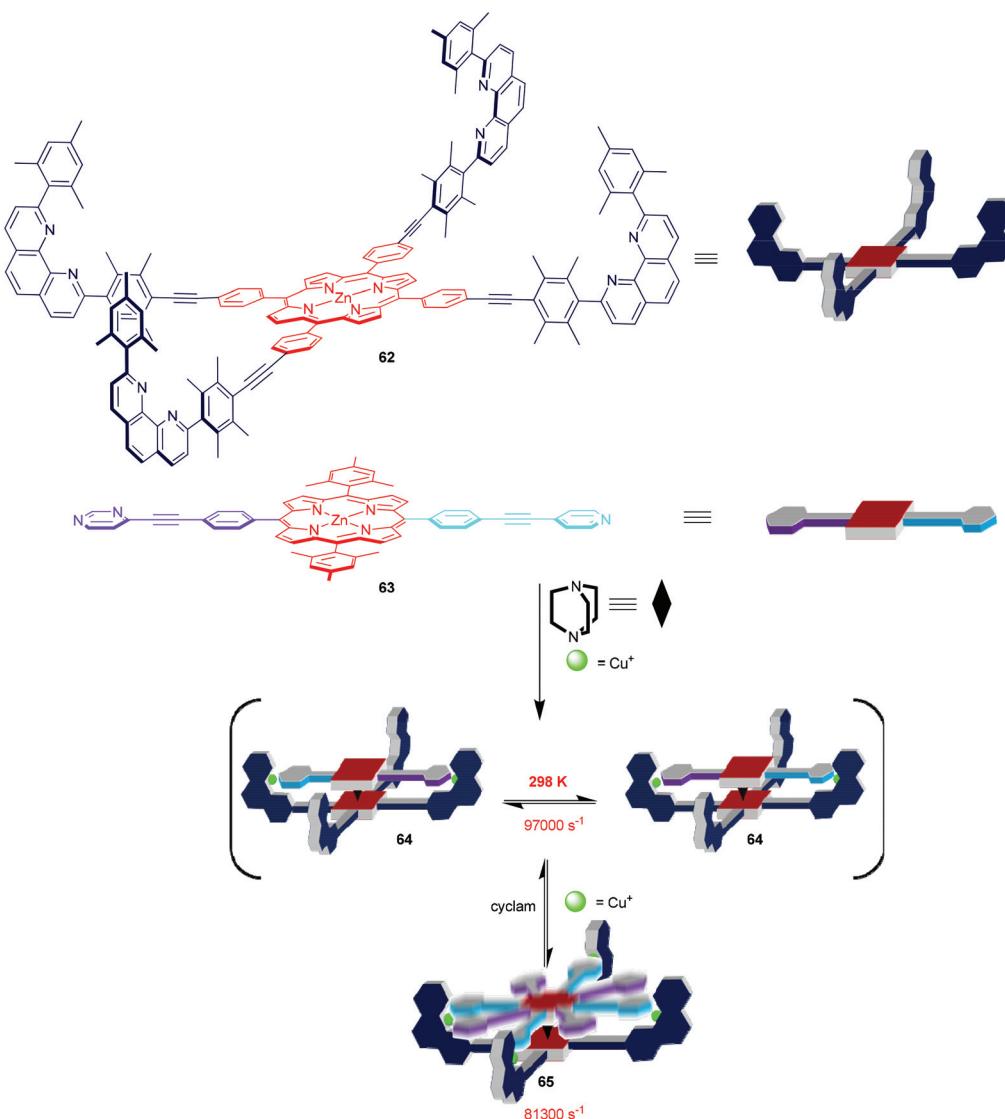
## 5. Conclusion

Ever since the birth of supramolecular chemistry, achieving superior structural features as well as efficacious functions

analogous to those in natural systems has been an immense challenge for chemists. To this end, our heteroleptic self-assembly protocols together with self-sorting represent a powerful tool for constructing demanding multicomponent supramolecules. Based on these newly available construction tools, we have elaborated in recent years a wide range of diverse multicomponent assemblies that exhibit interesting properties for various fields of application, such as *smart* materials, sophisticated nanomachines, switchable catalysis, *etc.* Efforts to extend our coordination tools even further to prepare aggregates with more than 7 components will be the focus of our laboratory in the years to come.

## Acknowledgements

We are indebted to the Deutsche Forschungsgemeinschaft (Schm 647/15-1 and 19-1), the Alexander von Humboldt foundation and the University of Siegen for financial support over many years. Moreover, we are most grateful to all coworkers and collaborators who contributed with great ideas, dedicated work and many publications for the advancement of our research in this field.

Scheme 13 Self-assembly of 4-component nanorotors **64** and **65**.<sup>80</sup>

## References

- (a) J.-M. Lehn, *Angew. Chem., Int. Ed. Engl.*, 1988, **27**, 89; (b) J.-M. Lehn, *Science*, 1993, **260**, 1762; (c) D. S. Lawrence, T. Jiang and M. Levett, *Chem. Rev.*, 1995, **95**, 2229.
- P. J. Stang, *J. Am. Chem. Soc.*, 2012, **134**, 11829.
- (a) S. J. Cantrill, K. S. Chichak, A. J. Peters and J. F. Stoddart, *Acc. Chem. Res.*, 2005, **38**, 1; (b) R. S. Forgan, J.-P. Sauvage and J. F. Stoddart, *Chem. Rev.*, 2011, **111**, 5434.
- T. K. Ronson, S. Zarra, S. P. Black and J. R. Nitschke, *Chem. Commun.*, 2013, **49**, 2476.
- (a) M. von Delius and D. A. Leigh, *Chem. Soc. Rev.*, 2011, **40**, 3656; (b) A. Coskun, M. Banaszak, R. D. Astumian, J. F. Stoddart and B. A. Grzybowski, *Chem. Soc. Rev.*, 2012, **41**, 19.
- (a) J.-M. Lehn, *Prog. Polym. Sci.*, 2005, **30**, 814; (b) T. F. A. de Greef and E. W. Meijer, *Nature*, 2008, **453**, 171; (c) T. F. A. De Greef, M. M. J. Smulders, M. Wolffs, A. P. H. J. Schenning, R. P. Sijbesma and E. W. Meijer, *Chem. Rev.*, 2009, **109**, 5687; (d) J.-M. Lehn, *Angew. Chem., Int. Ed.*, 2013, **52**, 2836.
- R. Chakrabarty, P. S. Mukherjee and P. J. Stang, *Chem. Rev.*, 2011, **111**, 6810.
- M. M. J. Smulders, I. A. Riddell, C. Browne and J. R. Nitschke, *Chem. Soc. Rev.*, 2013, **42**, 1728.
- M. Schmittel and K. Mahata, *Angew. Chem., Int. Ed.*, 2008, **47**, 5284.
- S. De, K. Mahata and M. Schmittel, *Chem. Soc. Rev.*, 2010, **39**, 1555.
- (a) R. Krämer, J.-M. Lehn and A. Marquis-Rigault, *Proc. Natl. Acad. Sci. U. S. A.*, 1993, **90**, 5394; (b) J.-M. Lehn and A. V. Eliseev, *Science*, 2001, **291**, 2331.
- (a) J.-P. Sauvage and J. Weiss, *J. Am. Chem. Soc.*, 1985, **107**, 6108; (b) J.-F. Nierengarten, C. O. Dietrich-Buchecker and J.-P. Sauvage, *J. Am. Chem. Soc.*, 1994, **116**, 375; (c) J. Frey,

C. Tock, J.-P. Collin, V. Heitz, J.-P. Sauvage and K. Rissanen, *J. Am. Chem. Soc.*, 2008, **130**, 11013.

13 (a) B. Hasenknopf, J.-M. Lehn, G. Baum and D. Fenske, *Proc. Natl. Acad. Sci. U. S. A.*, 1996, **93**, 1397; (b) V. C. M. Smith and J.-M. Lehn, *Chem. Commun.*, 1996, 2733.

14 M. Yoshizawa, M. Nagao, K. Kumazawa and M. Fujita, *J. Organomet. Chem.*, 2005, **690**, 5383.

15 L. Zhao, B. H. Northrop, Y.-R. Zheng, H.-B. Yang, H. J. Lee, Y. M. Lee, J. Y. Park, K.-W. Chi and P. J. Stang, *J. Org. Chem.*, 2008, **73**, 6580.

16 (a) K.-W. Chi, C. Addicott, A. M. Arif and P. J. Stang, *J. Am. Chem. Soc.*, 2004, **126**, 16569; (b) Y.-R. Zheng, Z. Zhao, M. Wang, K. Ghosh, J. B. Pollock, T. R. Cook and P. J. Stang, *J. Am. Chem. Soc.*, 2010, **132**, 16873.

17 M. Schmittel and V. Kalsani, *Top. Curr. Chem.*, 2005, **245**, 1.

18 (a) S. Ghosh, D. R. Turner, S. R. Batten and P. S. Mukherjee, *Dalton Trans.*, 2007, 1869; (b) O. V. Dolomanov, A. J. Blake, N. R. Champness, M. Schröder and C. Wilson, *Chem. Commun.*, 2003, 682.

19 (a) D. G. Cuttell, S.-M. Kuang, P. E. Fanwick, D. R. McMillin and R. A. Walton, *J. Am. Chem. Soc.*, 2002, **124**, 6; (b) Q. Zhang, J. Ding, Y. Cheng, L. Wang, Z. Xie, X. Jing and F. Wang, *Adv. Funct. Mater.*, 2007, **17**, 2983.

20 M. L. Saha, S. De, S. Pramanik and M. Schmittel, *Chem. Soc. Rev.*, 2013, **42**, 6860.

21 C. A. Hunter and H. L. Anderson, *Angew. Chem., Int. Ed.*, 2009, **48**, 7488.

22 (a) M. M. Safont-Sempere, G. Fernández and F. Würthner, *Chem. Rev.*, 2011, **111**, 5784; (b) K. Osowska and O. Š. Miljanić, *Synlett*, 2011, 1643; (c) M. L. Saha and M. Schmittel, *Org. Biomol. Chem.*, 2012, **10**, 4651.

23 M. Schmittel and A. Ganz, *Chem. Commun.*, 1997, 999.

24 M. Schmittel, A. Ganz, D. Fenske and M. Herderich, *J. Chem. Soc., Dalton Trans.*, 2000, 353.

25 (a) M. Schmittel, A. Ganz, W. A. Schenk and M. Hagel, *Z. Naturforsch., B: Chem. Sci.*, 1999, 559; (b) S. De, S. Pramanik and M. Schmittel, *Dalton Trans.*, 2013, **42**, 15391.

26 M. Schmittel and K. Mahata, *Chem. Commun.*, 2008, 2550.

27 M. Schmittel, A. Ganz and D. Fenske, *Org. Lett.*, 2002, **4**, 2289.

28 (a) M. Schmittel, H. Ammon, V. Kalsani, A. Wiegrefe and C. Michel, *Chem. Commun.*, 2002, 2566; (b) R. S. K. Kishore, V. Kalsani and M. Schmittel, *Chem. Commun.*, 2006, 3690.

29 M. Schmittel, V. Kalsani, D. Fenske and A. Wiegrefe, *Chem. Commun.*, 2004, 490.

30 (a) M. Schmittel, V. Kalsani and L. Kienle, *Chem. Commun.*, 2004, 1534; (b) M. Schmittel, V. Kalsani and J. W. Bats, *Inorg. Chem.*, 2005, **44**, 4115.

31 V. Kalsani, H. Bodenstedt, D. Fenske and M. Schmittel, *Eur. J. Inorg. Chem.*, 2005, 1841.

32 R. S. K. Kishore, T. Paululat and M. Schmittel, *Chem.-Eur. J.*, 2006, **12**, 8136.

33 V. Kalsani, H. Ammon, F. Jäckel, J. P. Rabe and M. Schmittel, *Chem.-Eur. J.*, 2004, **10**, 5481.

34 (a) J. Fan, J. W. Bats and M. Schmittel, *Inorg. Chem.*, 2009, **48**, 6338; (b) M. Schmittel, M. L. Saha and J. Fan, *Org. Lett.*, 2011, **13**, 3916; (c) J. Fan, M. L. Saha, B. Song, H. Schönher and M. Schmittel, *J. Am. Chem. Soc.*, 2012, **134**, 150.

35 Depending on the substituent in the 4-position of anilines, the association constant  $K_{\text{ass}}$  of iminopyridines towards  $[\text{Cu}(\text{phen}_{\text{Ar}2})]^+$  in  $\text{CH}_2\text{Cl}_2$  varies from  $10^4$  to  $10^6 \text{ M}^{-1}$ .

36 M. Schmittel, V. Kalsani, R. S. K. Kishore, H. Cölfen and J. W. Bats, *J. Am. Chem. Soc.*, 2005, **127**, 11544.

37 M. L. Saha and M. Schmittel, *J. Am. Chem. Soc.*, 2013, **135**, 17743.

38 M. Schmittel, V. Kalsani, P. Mal and J. W. Bats, *Inorg. Chem.*, 2006, **45**, 6370.

39 M. Schmittel and P. Mal, *Chem. Commun.*, 2008, 960.

40 M. Schmittel and B. He, *Chem. Commun.*, 2008, 4723.

41 M. Schmittel and K. Mahata, *Inorg. Chem.*, 2009, **48**, 822.

42 M. Schmittel and S. K. Samanta, *J. Org. Chem.*, 2010, **75**, 5911.

43 M. Schmittel, B. He, J. Fan, J. W. Bats, M. Engeser, M. Schlosser and H.-J. Deiseroth, *Inorg. Chem.*, 2009, **48**, 8192.

44 S. K. Samanta, D. Samanta, J. W. Bats and M. Schmittel, *J. Org. Chem.*, 2011, **76**, 7466.

45 (a) S. Neogi, G. Schnakenburg, Y. Lorenz, M. Engeser and M. Schmittel, *Inorg. Chem.*, 2012, **51**, 10832; (b) S. Neogi, Y. Lorenz, M. Engeser, D. Samanta and M. Schmittel, *Inorg. Chem.*, 2013, **52**, 6975.

46 D. Fiedler, D. H. Leung, R. G. Bergman and K. N. Raymond, *Acc. Chem. Res.*, 2005, **38**, 351.

47 K. Harris, D. Fujita and M. Fujita, *Chem. Commun.*, 2013, **49**, 6703.

48 For a detailed classification of completable self-sorting systems see ref. 22c.

49 (a) W. Jiang, H. D. F. Winkler and C. A. Schalley, *J. Am. Chem. Soc.*, 2008, **130**, 13852; (b) W. Jiang and C. A. Schalley, *Proc. Natl. Acad. Sci. U. S. A.*, 2009, **106**, 10425.

50 M. Schmittel, R. S. K. Kishore and J. W. Bats, *Org. Biomol. Chem.*, 2007, **5**, 78.

51 K. Mahata and M. Schmittel, *J. Am. Chem. Soc.*, 2009, **131**, 16544.

52 M. L. Saha, K. Mahata, D. Samanta, V. Kalsani, J. Fan, J. W. Bats and M. Schmittel, *Dalton Trans.*, 2013, **42**, 12840.

53 M. Schmittel and K. Mahata, *Chem. Commun.*, 2010, **46**, 4163.

54 K. Mahata and M. Schmittel, *Beilstein J. Org. Chem.*, 2011, **7**, 1555.

55 M. L. Saha, J. W. Bats and M. Schmittel, *Org. Biomol. Chem.*, 2013, **11**, 5592.

56 In the  $^1\text{H}$ -NMR characterisation of the library (Scheme 6a) the authors found some additional signals ( $\leq 8\%$ ) that represent the alternative heteroleptic complexes  $[\text{Zn}(16)(18)](\text{OTf})_2$  and  $[\text{Cu}(17)(26)](\text{PF}_6)$ .

57 K. Mahata, M. L. Saha and M. Schmittel, *J. Am. Chem. Soc.*, 2010, **132**, 15933.

58 J. R. Nitschke, *Nature*, 2009, **462**, 736.



59 M. D. Ward and P. R. Raithby, *Chem. Soc. Rev.*, 2013, **42**, 1619.

60 M. L. Saha, S. Pramanik and M. Schmittel, *Chem. Commun.*, 2012, **48**, 9459.

61 (a) M. Schmittel, S. De and S. Pramanik, *Angew. Chem., Int. Ed.*, 2012, **51**, 3832; (b) M. Schmittel, S. Pramanik and S. De, *Chem. Commun.*, 2012, **48**, 11730.

62 M. Schmittel, P. Mal and A. de los Rios, *Chem. Commun.*, 2010, **46**, 2031.

63 S. K. Samanta and M. Schmittel, *Org. Biomol. Chem.*, 2013, **11**, 3108.

64 (a) K. Nomoto, S. Kume and H. Nishihara, *J. Am. Chem. Soc.*, 2009, **131**, 3830; (b) S. Kume, K. Nomoto, T. Kusamoto and H. Nishihara, *J. Am. Chem. Soc.*, 2009, **131**, 14198; (c) S. Kume and H. Nishihara, *Chem. Commun.*, 2011, **47**, 415; (d) M. Nishikawa, K. Nomoto, S. Kume and H. Nishihara, *J. Am. Chem. Soc.*, 2012, **134**, 10543; (e) M. Nishikawa, S. Kume and H. Nishihara, *Phys. Chem. Chem. Phys.*, 2013, **15**, 10549.

65 (a) Y. Pellegrin, M. Sandroni, E. Blart, A. Planchat, M. Evain, N. C. Bera, M. Kyanuma, M. Sliwa, M. Rebarz, O. Poizat, C. Daniel and F. Odobel, *Inorg. Chem.*, 2011, **50**, 11309; (b) M. Sandroni, M. Kyanuma, A. Planchat, N. Szwarski, E. Blart, Y. Pellegrin, C. Daniel, M. Boujtia and F. Odobel, *Dalton Trans.*, 2013, **42**, 10818.

66 (a) F. Sozmen, B. S. Oksal, O. A. Bozdemir, O. Buyukcakir and E. U. Akkaya, *Org. Lett.*, 2012, **14**, 5286; (b) M. G. Fraser, H. van der Salm, S. A. Cameron, A. G. Blackman and K. C. Gordon, *Inorg. Chem.*, 2013, **52**, 2980.

67 Y. Fang, T. Murase, S. Sato and M. Fujita, *J. Am. Chem. Soc.*, 2013, **135**, 613.

68 (a) M. Frank, J. M. Dieterich, S. Freye, R. A. Mata and G. H. Clever, *Dalton Trans.*, 2013, **42**, 15906; (b) S. Freye, R. Michel, D. Stalke, M. Pawliczek, H. Frauendorf and G. H. Clever, *J. Am. Chem. Soc.*, 2013, **135**, 8476; (c) S. Freye, D. M. Engelhard, M. John and G. H. Clever, *Chem.-Eur. J.*, 2013, **19**, 2114.

69 M. Schmittel, B. He and P. Mal, *Org. Lett.*, 2008, **10**, 2513.

70 (a) V. W.-W. Yam and K. K.-W. Lo, *Chem. Soc. Rev.*, 1999, **28**, 323; (b) S. Sculfort and P. Braunstein, *Chem. Soc. Rev.*, 2011, **40**, 2741; (c) H. Xiang, J. Cheng, X. Ma, X. Zhou and J. J. Chruma, *Chem. Soc. Rev.*, 2013, **42**, 6128.

71 M. E. Carnes, M. S. Collins and D. W. Johnson, *Chem. Soc. Rev.*, 2014, DOI: 10.1039/c3cs60349k.

72 A. Aderem, *Cell*, 2005, **121**, 511.

73 (a) V. Balzani, A. Credi and M. Venturi, *Molecular Devices and Machines*, Wiley-VCH, Weinheim, 2nd edn, 2008; (b) B. L. Feringa and W. R. Browne, *Molecular Switches 1 + 2*, Wiley-VCH, Weinheim, 2nd edn, 2011.

74 K. Parimal, E. H. Witlicki and A. H. Flood, *Angew. Chem., Int. Ed.*, 2010, **49**, 4628.

75 (a) G. C. Conant and A. Wagner, *Genome Biol.*, 2005, **6**, R50; (b) S. Pasek, J.-L. Risler and P. Brézellec, *Bioinformatics*, 2006, **22**, 1418.

76 G. R. Whittell, M. D. Hager, U. S. Schubert and I. Manners, *Nat. Mater.*, 2011, **10**, 176.

77 K. Kinbara and T. Aida, *Chem. Rev.*, 2005, **105**, 1377.

78 U. Lüning, *Angew. Chem., Int. Ed.*, 2012, **51**, 8163.

79 (a) R. Hernandez, H.-R. Tseng, J. W. Wong, J. F. Stoddart and J. I. Zink, *J. Am. Chem. Soc.*, 2004, **126**, 3370; (b) H. Kai, S. Nara, K. Kinbara and T. Aida, *J. Am. Chem. Soc.*, 2008, **130**, 6725; (c) S. Hiraoka, Y. Hisanaga, M. Shiro and M. Shionoya, *Angew. Chem., Int. Ed.*, 2010, **49**, 1669.

80 S. K. Samanta and M. Schmittel, *J. Am. Chem. Soc.*, 2013, **135**, 18794.

